Cooperativity of self-organized Brownian motors pulling on soft cargoes

Javier G. Orlandi,* Carles Blanch-Mercader, Jan Brugués, and Jaume Casademunt
Departament d'Estructura i Constituents de la Matèria, Facultat de Física, Universitat de Barcelona, Avinguda Diagonal 647, E-08028 Barcelona, Spain

(Received 5 August 2010; revised manuscript received 1 October 2010; published 7 December 2010)

We study the cooperative dynamics of Brownian motors moving along a one-dimensional track when an external load is applied to the leading motor, mimicking molecular motors pulling on membrane-bound cargoes in intracellular traffic. Due to the asymmetric loading, self-organized motor clusters form spontaneously. We model the motors with a two-state noise-driven ratchet formulation and study analytically and numerically the collective velocity-force and efficiency-force curves resulting from mutual interactions, mostly hard-core repulsion and weak (nonbinding) attraction. We analyze different parameter regimes including the limits of weak noise, mean-field behavior, rigid coupling, and large numbers of motors, for the different interactions. We present a general framework to classify and quantify cooperativity. We show that asymmetric loading leads generically to enhanced cooperativity beyond the simple superposition of the effects of individual motors. For weakly attracting interactions, the cooperativity is mostly enhanced, including highly coordinated motion of motors and complex nonmonotonic velocity-force curves, leading to self-regulated clusters. The dynamical scenario is enriched by resonances associated to commensurability of different length scales. Large clusters exhibit synchronized dynamics and bidirectional motion. Biological implications are discussed.

DOI: 10.1103/PhysRevE.82.061903 PACS number(s): 87.17.Aa, 87.16.Nn, 87.10.−e, 05.40.−a

I. INTRODUCTION

The collective behavior of molecular motors plays a central role in a large variety of active processes in cell biology [1–3]. While the essential physical mechanisms underlying individual molecular motor function are now well understood within a general perspective in nonequilibrium physics [4–7], it has been emphasized that complex emerging phenomena occur when interacting motors act collectively, such as bidirectional motion, oscillations, hysteresis, or the formation of dynamical structures [8–11]. Motors often act in large assemblies, such as in the so-called "rower" motors. In other instances, the so-called "porter" motors, which are usually in charge of transport in intracellular traffic, work either individually or in relatively small groups, typically less than ten. These motors, such as conventional (dimeric) kinesins, are processive, that is, they perform a large number of steps before detaching from the track filament. Typically, processive motors have more difficulty to work collectively than individually because the presence of other motors can interfere in their cycle [11]. A typical collective task of processive motors is the transport of vesicles over long distances [12]. To that purpose, small groups of motors are required to control the distance to be traveled by the vesicle, which depends on the number of motors linked to its membrane through the detailed regulation of the kinetics of binding or unbinding between motors and the microtubule [13]. In such cases, the detailed interactions between motors may not be relevant. In recent studies, however, it has been shown that the coordinated action of groups of kinesins must be invoked to explain some tasks that require relatively large forces, such as the formation of membrane tubes [14–21]. The situation where processive motors pull on soft cargoes, such as vesicles or membrane tubes, differs fundamentally from most commonly studied cases of motors attached to rigid cargoes, because—due to the fluidlike nature of the membrane—the motors cannot exert tangential forces to the cargo, with the friction with the membrane being negligible. Since the cargo is also deformable, motors can cluster at the front regions where a normal component can be exerted (see discussion in Ref. [18]). For geometrical reasons, this limits to relatively small numbers of motors per track. In the experiments of conventional kinesin pulling on tubes it has been shown that two to four motors per track are sufficient to explain the observations [18]. In a previous work [17] it has been argued that the ability to transmit force at a finite velocity by conventional kinesin along a single track in the pulling-tube arrangement could saturate with the number of motors for relatively small numbers of them. These studies raise the question on the extent to which motors are capable to transmit forces through their direct motor-motor interactions, that is, to add up their individual contributions to the overall force on the cargo.

In studies of rigidly or elastically coupled motors, their strong coupling has been shown to lead to nontrivial collective effects [4,9,11]. In particular, it has been pointed out that motors can become highly cooperative by increasing the overall velocity and the overall force, but also undertaking tasks more efficiently. The situation in transport of soft cargoes, however, is fundamentally different in that the motors are free to move with respect to each other and that the external force is asymmetrically loaded, that is, the external load in unequally applied to the motors. The combination of geometrical and mechanical constraints gives rise to a dynamical self-organizing mechanism: the trailing motors, because they are unloaded, will move faster than the loaded ones in front, and thus accumulate behind them. A motor cluster will dynamically form, and its collective behavior will depend strongly not only on the motor-motor interactions but also on the external force that ultimately controls

*orlandi@ecm.ub.es

the cohesion of the cluster. Even though attractive interactions may be present, the motor cluster is a self-organized dynamical structure, not a motor assembly resulting from the physical interactions.

The effect of interactions on the collective velocity-force curves in such an arrangement was first studied in Ref. [17], based on discrete Monte Carlo simulation and exact calculations based on a generalized asymmetric simple exclusion process (ASEP) formalism. There it was pointed out that the collective velocity-force curves were strongly sensitive to motor interactions and that strong deviations from naive superposition of the effects of individual motors are to be expected. The discrete ASEP approach gives an interesting perspective from the physics of nonequilibrium phase transitions [22–24] and is advantageous with respect to Langevin continuum formulations in that it allows remarkable analytical insights and is computationally very efficient. However, it may be problematic when generic motor-motor interactions other than excluded volume are expected to play a crucial role, because the effect of interactions is indirectly encoded in stochastic transition rates in a phenomenological way that is not easily correlated *a priori* to actual interaction potentials between motors. This is particularly important when more than two motors are involved, as in the closely packed clusters formed under unequal loading. To clarify this point and to make connection with other studies of collective motors where the Langevin picture has been illuminating [8–10], the problem was later addressed with this other perspective in Ref. [25], following the tentative discussion of this alternative already initiated in [17].

The Langevin formulation is a more mechanistic approach where the internal-state degrees of freedom of motors, related to conformational changes, are resolved and coupled to positional degrees of freedom through explicit arbitrary interaction potentials. Concepts such as force transmission and energetic efficiency are thus more naturally incorporated. In particular it allows us to explore the approach to the limits of mean field (MF) or rigid coupling motors, which have been previously studied. The present paper expands and generalizes the approach presented in Ref. [25], where nontrivial cooperative effects of Brownian motors where discussed, often with dramatic effects in the collective velocity-force curves and in the efficiency curves. We now include analytical results that complete the study from a theoretical point of view and generalize and complete the numerical simulations with more general ratchet models to identify and understand the underlying physical mechanisms of cooperativity and its degree of universality. The study transcends the biological motivation into the more general context of Brownian motors and nonequilibrium transport [4,6,26–28]. We will focus on motors that are driven by noise, a situation that may be considered as particularly inefficient when acting individually, but which will turn highly cooperative under unequal loading. In the biological context, several types of molecular motors have been identified that are well modeled by a noise-driven ratchet mechanism, typically in the monomeric kinesin subfamily, most remarkably the so-called KIF1A, a motor that is responsible for vesicle transport in axons [29–31]. In this paper we will not only address the general problem of noise-driven motors under unequal loading, but will also address the implications for the parameter ranges relevant to specific biological motors. The question is of significant importance in biology since axonal traffic disorders are known to be associated to many neurodegenerative diseases [32]. Because of its specific high demands of long distances, high speeds, and large forces, axonal trafficking requires the cooperative action of groups of motors. This suggests that a high cooperativity of noise-driven motors pulling on soft cargoes could be a key reason why axonal vesicle transport is specifically carried out by these type of motors such as monomeric kinesins, which—when taken individually—are clearly outperformed by conventional (dimeric) kinesins.

Layout and summary of results

In Sec. II we set forth the theoretical framework that serves as basis for the subsequent discussion. We first define our mathematical model (Sec. II A) and discuss the rationale of a Langevin continuous formulation in comparison with a common alternative approach based on discrete Monte Carlo random walkers (Sec. II B). In Sec. II C we define a mean-field approximation and discuss its predictions for the collective behavior of motor clusters under unequal loading. We also introduce some explicit criteria of validity of this approximation. The mean-field behavior defined here provides a suitable basis to classify the different possible scenarios of cooperativity. Finally, in Sec. II D we provide some exact results for the one-motor problem and for the mean-field approximation.

Section III is devoted to the case of repulsive interaction between motors. In Sec. III A we focus on the case of short-range excluded volume repulsion. We recover and generalize the results of enhanced cooperativity reported in Ref. [25], now for the case of general asymmetry of the potential. We discuss the mechanism that is responsible for the generic enhancement of cooperativity and, using the exact results for the mean-field case, we show how this enhancement becomes dramatically pronounced in the weak-noise limit. In this section we also show the origin of the exceptional phenomenon of reduced cooperativity when the hard-core size of the motor becomes commensurate with the potential period, and we show that this may lead in some cases to nonmonotonic velocity-force curves, a phenomenon first encountered for attractive interactions in Ref. [25], but that may also occur for purely repulsive interactions. The convergence with the number of motors of the velocity-force curves to a single curve that exhibits extensive scaling of the force with the number of motors at a given velocity is discussed only for the fully asymmetric potential, while the generic case is postponed to Sec. VII. In Sec. III B we supply some exact results for the two-motor problem in the limit of vanishing noise intensity that prove the phenomenon of enhanced cooperativity for broad ranges of parameters. These results prove that for the fully asymmetric ratchet potential, the two-motor problem exhibits finite velocity, finite power, and finite efficiency in the strict limit of vanishing noise intensity, provided that the external force is unequally loaded, thus isolating the cooperativity mechanism and illus-

trating its deterministic nature. Some proofs are sketched and some results are stated without proof. Finally, in Sec. III C we show explicitly the convergence to the mean-field limit when the range of the repulsive potential is increased and also for hard-core repulsion when the noise strength is increased.

In Sec. IV we analyze the case of attractive interactions. We first discuss the case of rigid elastic coupling as a reference case and then generalize the results of Ref. [25] of nonmonotonic force-velocity curves. We discuss the implications of this behavior for the dynamical selection of the number of motors in the cluster in terms of the external force and show that for arbitrary asymmetry of the ratchet potential the problem is remarkably richer, but that the different behaviors can be interpreted in terms of commensurability effects between the different length scales involved.

The effects of cooperativity in the collective efficiency of the system are addressed in Sec. V. It is shown that the global efficiency increases in general with the number of motors, generalizing the results of Ref. [25]. In particular we discuss the role of the degree of coordination of the cycles of the motors in the cluster. This becomes optimal at the larger speeds in the case of attractive interactions. In this case, we also show that the efficiency increases monotonically with the force if the number of motors is suitably selected.

In Sec. VI we briefly address the nontrivial effects associated to the commensurability of the different length scales of the ratchet potential and the mean motor distance, leading to rather exotic dynamical behaviors. The dynamics of large clusters are treated in Sec. VII, where we analyze the structure, force distribution, and synchronization of the motor clusters. In particular we discuss how new phenomena can emerge for large clusters, such as the occurrence of stochastic transitions between two velocities, one positive and one negative, a phenomenon that had been previously observed in rigid assemblies of motors. Finally, in Sec. VIII we discuss the implications for biological motors, in particular concerning the monomeric kinesion KIF1A, and we present an overview of the results obtained in Sec. IX.

II. THEORY OF COOPERATIVITY

A. Formulation of the problem: Minimal model

We consider a set of N motors moving along a one-dimensional track. An external force F opposing the motion is applied only to the foremost motor. For simplicity, and to better isolate the cooperative mechanisms, the motors are assumed infinitely processive, that is, they perform steps indefinitely along the track without detaching from it. This assumption may not be realistic for some biological applications but can be easily relaxed at a later stage of the research, once the cooperative mechanisms have been clarified [33]. We assume that motors interact with an arbitrary (nonbinding) potential. In all cases the potential will have a hard-core repulsive part of size σ, the motor size, which in general does not need to coincide with the period of the track. Here, we will consider a two-state ratchet model that is a slightly simplified version of the generic model of Ref. [4], yet more general than the case studied in Ref. [25]. The model is defined by a set of Langevin equations for the positions x_i of the N motors:

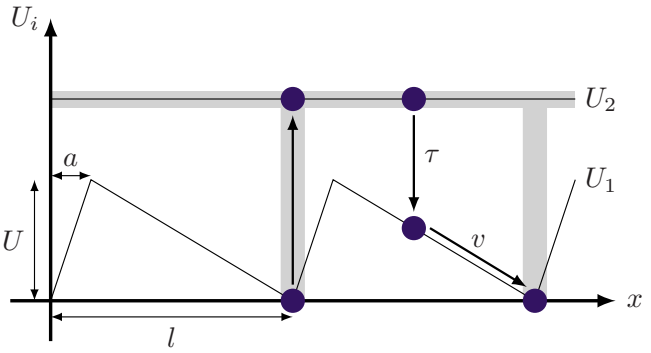

FIG. 1. (Color online) Piecewise linear potential for the motor-track interaction. Gray—the zone where transitions are allowed: localized and instantaneous from U_1 to U_2 and delocalized after a time τ from U_2 to U_1. See more details in the text.

$$\lambda \dot{x}_i = -U_i'(x_i,k_i) - \sum_{k\neq i} W'(x_i - x_k) - F\delta_{1i} + \zeta_i(t), \qquad (1)$$

where $i=1,\ldots,N$. k_i are discrete stochastic variables that label the two internal states of each motor, characterized by a strongly bound state with a potential $U_i(x_i,1)$ and a weakly bound state with a potential $U_i(x_i,2)$. $W(\xi)$ is the interaction potential between motors. In addition to the unequal loading, this setup differs fundamentally from some studies of collective Brownian motors, such as in Refs. [34,35], in that the switching between states is not simultaneous for all motors (flashing ratchet), but it occurs independently for each motor. The friction coefficient λ is assumed to be the same for the two states, so thermal noise is described by a Gaussian white process with autocorrelation,

$$\langle \zeta_i(t)\zeta_j(t')\rangle = 2k_BT\lambda\delta_{ij}\delta(t-t'), \qquad (2)$$

and defining a noise strength with the dimensions of a diffusion coefficient,

$$D \equiv k_BT/\lambda. \qquad (3)$$

We assume a generic piecewise asymmetric linear potential $U_i(x,1)$ (hereinafter, the U_1 state), like the sawtooth potential plotted in Fig. 1, with period ℓ, height U, and asymmetry a/ℓ. We define a sliding velocity $v \equiv U/\lambda(\ell-a)$. The state $U_i(x,2)$ (hereinafter, the U_2 state) is a weakly bound state that we model for simplicity as a flat potential. Excitations from U_1 to U_2 are localized at the minimum of U_1. This corresponds to a far-from-equilibrium condition $\Delta\mu \gg k_BT$, where for the case of biological motors $\Delta\mu$ is typically the chemical potential difference for adenosine triphosphate (ATP) hydrolysis. Consistently, thermal activation is neglected [4,26]. For simplicity we also assume that the excitation to the U_2 state is instantaneous upon reaching the minimum of U_1. This condition could be easily relaxed to account for a finite dwell time at the ATP-binding site, which in biological motors may not be negligible. This would complicate the analysis with an extra parameter, but would offer no qualitative changes unless this additional time scale be-

comes comparable or even larger than the others involved, a case that will be specifically addressed elsewhere [33] (see also Sec. VIII). Finally, we assign a finite lifetime τ to the diffusive state U_2. Deexcitations from that state are spatially delocalized. A natural assumption would be that the deexcitation rate was constant, implying an exponentially distributed decay time. For simplicity, however, throughout this paper we will assume that the decay time is not distributed, but is a fixed value τ. This assumption simplifies significantly the analytical calculations and the form of the final expressions, while it does not introduce any new physics [36]. In particular it allows us to find exact nontrivial solutions for the two-motor problem. The simulations reported here are also carried out in this case, but we have checked that an exponentially distributed decay time makes no qualitative difference. In some cases, we also consider an additional simplification by neglecting thermal noise in the U_1 state, the one that is deterministically dominated. This assumption will also simplify the final expressions of the single-motor problem and is justified in the weak-noise limit. The model with this additional assumption will be referred to as the minimal model. In general we will not neglect noise in the U_1 state unless otherwise indicated.

The problem has three relevant dimensionless parameters, which we group as

$$\alpha \equiv \frac{v\tau}{\ell - a}, \tag{4}$$

the ratio of the lifetime of U_2 to the characteristic sliding time in U_1;

$$\beta \equiv \frac{\ell}{\sqrt{4D\tau}}, \tag{5}$$

the ratio of the track period to the diffusive length in U_2; and the asymmetry parameter

$$\bar{a} \equiv \frac{a}{\ell}. \tag{6}$$

Our main observables will be the cluster velocity, defined as $V_N(F)=\langle \dot{x}_1 \rangle$, and the collective efficiency [26], which in the biological context reads

$$\eta_N(F) = \frac{FV_N(F)}{r_N(F)\Delta\mu}, \tag{7}$$

where $r_N(F)$ is the reaction rate, in our case the total number of excitations per unit time for all the motors. In some expressions we will use the dimensionless force

$$f \equiv \frac{F}{\lambda v}. \tag{8}$$

B. Rationale of continuous versus discrete approaches

Two different stochastic approaches have been proposed so far to deal with the problem at hand. One is based on generalizations of the so-called ASEP, proposed in Ref. [17] and developed later in Refs. [18,20], where motors perform a biased random walk in a one-dimensional lattice. The corresponding systems are then modeled as a discrete master equation well fitted to Monte Carlo simulation. This formalism is convenient to numerical simulation and also to analytical treatment and has been widely used in a more general context of nonequilibrium physics. On the other hand, the alternative continuous Langevin approach presented in the previous section, also introduced in Ref. [17] and later developed in Ref. [25], has some conceptual advantages for the problem at hand. Although the two formalisms can be made equivalent in principle in a sufficiently general formulation, in their simplest and practical formulations (with small number of parameters), they are not, and may yield significantly different results. In some aspects the comparison between the physics built in the model is not simple, in particular with regard to the nature of the interactions and the rules of force distribution.

In the biological context, the Langevin approach discussed here builds on the implicit assumption that the motor-motor interaction and the motor-track interaction can be treated separately, so that the force acting on a given motor is the superposition of both. That is, it assumes that the coarse-grained mechanistic view of the two-state models for a single motor can now be assumed to be valid for two interacting motors, and eventually for N, just adding a position-dependent interaction potential between them. This is not obvious since both effective interactions are phenomenological and are meant to result from some coarse-graining procedure, which in principle should be carried out jointly for the N-body problem, and in general it is different for each N. The alternative physical picture of the ASEP approach implicitly involves an opposite complementary view, one in which the presence of the second motor interferes with the first motor in a way that is more complicated than just adding a force. Since an explicit coarse graining of the two-motor problem cannot be carried out explicitly, this second view postulates some phenomenological hopping rates that are designed to properly encode the interactions. In its simplest formulation [17], the presence of a second motor next to the first modifies the hopping rates of the first, but the presence of a third motor does not. Consequently, this formulation then reduces the N-body statistics to the two-motor problem. The physical idea behind this assumption is that additional motors do not transmit force to the first directly, but they contribute to the collective behavior through an entropic repulsion (i.e., a third motor modifies the motion of the first motor by changing the statistics of the encounters between the first and second motors). This entropic force must eventually saturate with N, as found in [17], implying that adding more motors to a cluster has eventually no effect. In fact, in the lattice model of [17], the velocity-force curves for different N's all converge to a single curve independent of N for large N. On the contrary, in the Langevin two-state model, the mechanical force between motors is explicit, and in addition to entropic repulsion, there is direct force transmission built in. Then it may be expected that the total force exerted by the cluster is extensive with the number of motors. In Ref. [25], for instance, we showed in a simple case that the velocity-force curves for large N collapsed to a single curve when the force was scaled by N [37].

One of the advantages of the Langevin approach is that the treatment of interactions is more transparent and versatile. It allows us to easily interpolate between weakly interacting motors and rigid coupling, for instance, or to simply approach a mean-field limit increasing the range of the potential. It is illustrative to remark the different meaning of "attractive" interactions in Refs. [17,25]. The way an effective attraction is modeled in the discrete model of [17] does not correspond to a potential with an attractive part in the Langevin formulation since it contains no action-reaction principle. It precludes the possibility that the leading motor pulls on the trailing one. The result of two "attracting" motors is then opposed in the two scenarios. In the Langevin model it enhances cooperativity even more than with hard-core repulsion, while in the discrete model it reduces it.

In general, which one of the two approaches does capture best the collective behavior of a real problem is an issue that must be addressed on a case-by-case basis. For the case of monomeric (one-headed) kinesin, for instance, we propose that a ratchet model is appropriate and can account for observed collective behavior. In this case we expect that force transmission holds for large numbers of motors. For conventional (two-headed) kinesin, instead, a model with limited force transmission might be more adequate.

C. Mean-field theory and cooperativity

1. Predictions of the mean-field ansatz

The collective velocity-force curves for the general Eq. (1) can be solved exactly within a MF ansatz, which may not be justified in general but provides the right behavior for sufficiently long-ranged interactions and/or sufficiently large noise intensity. Within the MF approach, the N-motor problem will reduce formally to the single-motor problem. In this context, our MF ansatz consists of approximating the total force exerted to each motor from the other motors at any time, with the average steady-state value, that is, $W'(x_i-x_k) \simeq \langle W'(x_i-x_k)\rangle$. This approximation preserves the correlations between positional and internal degrees of freedom for each single motor, but neglects correlations between positional and internal degrees of freedom of different motors [38]. Then, all the equations get decoupled, and each motor is subject to a constant force. Since in the steady state all motors of the cluster must move at the same speed, all constant-force terms in the equations must be equal and add up to the external force F, so each motor is subject to a net force F/N. The MF prediction for the collective velocity-force curve then reads

$$V_N^{MF}(F) = V_1(F/N), \tag{9}$$

that is, each motor in the cluster moves with the speed that it would have if isolated and being loaded with its equal share of the total force F/N. Notice that the above expression makes no assumption on the nature of the single-motor problem, which may be treated exactly and thus exhibit complex nonlinear behavior. In the particular case of a linear velocity-force for the single-motor problem, the MF velocity coincides with the velocity of the center of mass of a set of independent motors, with $N-1$ of them free and one loaded with the total force.

Similarly, the MF ansatz implies that, at a given speed, a motor cluster is exerting a total force F_N, which is N times the force of a single motor at the same speed:

$$F_N^{MF}(V) = NF_1(V). \tag{10}$$

We call this equation the condition of exact extensivity of the force.

With regard to the collective efficiency of motor clusters, the MF ansatz also yields simple relations, such as the exact extensivity of the reaction rate, $r_N^{MF}(F)=Nr_1(F/N)$, which in turn reduces the collective efficiency of N motors to that of a single motor with its share of the force, that is,

$$\eta_N^{MF}(F) = \eta_1(F/N). \tag{11}$$

Consequently, within MF the efficiency at a given velocity $\eta(V)$ does not depend on the number of motors. Motors do cooperate in the sense that they add their forces to maintain a certain velocity, but there is no gain in efficiency by working together. In the biological context this means that, at a given speed, the work obtained per each hydrolyzed ATP molecule is fixed regardless of N.

2. Criteria of validity of the mean-field approximation

The validity criteria of the MF approximation involve both the type of motor-motor interactions and the strength of the noise. Here, we will restrict the discussion to the two-motor problem, but the extension is trivial. The general criterion for the validity of MF imposes conditions on the mean value $\xi_0=\langle\xi\rangle\equiv\langle x_1-x_2\rangle$ of the distance between motors ξ and its fluctuations. The equation for the relative coordinate can be written as

$$\lambda\dot{\xi} = -U_1'(x_1,t) + U_2'(x_2,t) - 2W'(\xi) - F + \zeta_r(t), \tag{12}$$

with

$$\langle\zeta_r(t)\zeta_r(t')\rangle = 4k_BT\lambda\delta_{ij}\delta(t-t'). \tag{13}$$

For repulsive interactions, the scale ξ_0 is fixed by the balance between the repulsive force and the effective attraction associated to the term $-F$ due to the unequal loading. The MF ansatz is expected to be valid if for the typical scale of variation of ξ the interaction force between motors does not change significantly. If the noise is weak, this poses a condition on the potential. In fact, in this limit ξ_0 is given by the minimum of the effective potential $2W(\xi)+F\xi$, and the force between motors $W'(\xi)$ will be approximately constant around the value $-F/2$ provided that the minimum of the effective potential is sufficiently flat at the scale ℓ where correlations due to the terms $U_1'(x_1,t)$ and $U_2'(x_2,t)$ are built. This yields the condition $\ell|W''(\xi_0)/W'(\xi_0)|\ll 1$, where ξ_0 depends on F through the condition $-W'(\xi_0)=F/2$. Obviously we are also implicitly assuming that $\xi_0\gg\ell$. For a potential with an exponential tail of range Λ, the conditions for the second derivative of the potential and for the range of interaction are the same and reduce to $\Lambda\gg\ell$ and $\Lambda\gg\sigma$. For hard-core repulsion, however, the condition for the smoothness of the potential is not satisfied, so strong deviations

from MF are to be expected in the weak-noise limit.

The validity of MF may also be achieved for sufficiently large noise intensities. For a long-range repulsive potential, we consider the estimation of the fluctuations $\langle \delta\xi^2 \rangle$ around the minimum ξ_0 of the effective potential $2W(\xi)+F\xi$ that results from neglecting the terms $-U_1'(x_1,t)+U_2'(x_2,t)$ in Eq. (12). This yields $\langle \delta\xi^2 \rangle \sim 2D\lambda/W''(\xi_0)$. If we assume MF then the average of $-U_1'(x_1,t)+U_2'(x_2,t)$ is zero, so requiring that $2D\lambda/W''(\xi_0) \gg \ell^2$ poses a self-consistency criterion for MF. In the case of an exponential decay of $W(\xi)$, and using $-W'(\xi_0)=F/2$, the condition reads $\frac{4D\lambda}{F\ell}\frac{\Lambda}{\ell} \gg 1$, which is satisfied by a long-ranged potential even if the thermal energy $D\lambda=k_BT$ is not much larger than the energy scale $F\ell$.

Finally, for a short-ranged repulsion we may still reach the MF limit at sufficiently strong noise. In fact, for hard-core repulsion with strong noise, most of the time the motors are not in contact, so if we replace $-U_1'(x_1,t)+U_2'(x_2,t)-F$ with its average, which reduces to $\lambda[V_1(F)-V_1(0)] \equiv -\lambda\Delta V(F)$ when motors do not interact, then the separation between motors by entropic repulsion is distributed exponentially with a decay length $2D/\Delta V(F)$. A self-consistency criterion for MF can thus be obtained by imposing this length to be larger than ℓ, that is, $2D/\ell\Delta V(F) \gg 1$.

In situations that combine finite noise strength and finite potential range it is not simple to estimate *a priori* the validity of the MF approximation. As a general rule, MF may be achieved by increasing either the noise strength or the range of the repulsive potential, but the convergence to the MF will be nonuniform, i.e., dependent on F. In Sec. III C we explicitly address this F-dependent convergence in an illustrative example combining a hard-core plus an exponential tail with finite noise intensity.

3. Classification of cooperativity

The naive collective behavior predicted by the MF theory may be called "neutral cooperativity." As already mentioned, motors do cooperate in the sense that they simply add forces to the cluster, but there is no gain in the collective efficiency. For the original problem, however, MF will not hold in general, and significant deviations from its predictions are expected. Remarkably, as reported in Ref. [25], typical deviations from the MF equalities happen to be in the direction where cooperativity is enhanced, that is,

$$V_N(F) > V_1(F/N), \tag{14}$$

$$F_N(V) > NF_1(V), \tag{15}$$

$$r_N(F) < Nr_1(F/N). \tag{16}$$

These three conditions are not strictly equivalent in general, but they do usually occur together except for very special cases. As we will see in Sec. V, the reaction rate r_N is appropriate to quantify the degree of coordination of motors. One may define a compact criterion for "enhanced cooperativity" through the condition for the efficiency

$$\eta_N(F) > \eta_1(F/N). \tag{17}$$

Remarkably, as we will see, the enhancement of cooperativity can be quantitatively very strong in some parameter regimes, typically for weak noise. On the contrary, we will also see that the opposite inequality happens very rarely, typically for very narrow ranges of parameters. Furthermore, whenever cooperativity is reduced, the deviations from MF are quantitatively small. The generic scenario for motors based on a Brownian ratchet mechanism is thus that of enhanced cooperativity. That is, when a force is applied to one of them, other motors team up to work out more efficiently than they would do if separated. In the biological context, this means that there will be a net gain of mechanical work for each molecule of ATP that is hydrolyzed.

D. Exact solution of the one-motor (MF) problem

For further reference we obtain here some exact expressions for the single-motor problem, which yield automatically the MF approximation to the N-motor problem with the substitution $F \to F/N$. It is useful to solve the minimal model that exhibits the simplest possible explicit expressions for the different observables, in particular for the velocity-force and efficiency-force relations. For the minimal model defined in Sec. II A, in its fully asymmetric version ($a=0$), the stall force and the velocity at zero load take a very simple form that we will use as a reference and for normalization purposes. They are both independent of noise strength D and read, respectively [25],

$$F_s^0 = \lambda v \min\left[1, \frac{1}{2\alpha}\right], \tag{18}$$

$$V_1^0(0) = \frac{v}{1+2\alpha}. \tag{19}$$

If the noise is not neglected in the U_1 state then the above results correspond to the weak-noise limit.

Note that the velocity at zero load remains finite at $D=0^+$ due to the fact that $a=0$. These results can be easily obtained from simple arguments, taking advantage of the constant decay time. Under these conditions, the exact velocity-force curve for the minimal model with arbitrary a can be obtained. The general expression and its derivation are given in Appendix A. For the particular case of $a=0$, in terms of the dimensionless force, $f \equiv F/(\lambda v)$, it takes the form

$$V_1^0(F) = v(1-f)\frac{\phi(f)}{\alpha+\phi(f)}, \tag{20}$$

where

$$\phi(f) \equiv \phi(\alpha,\beta,f) = \frac{1}{2} - \frac{\alpha\beta}{\sqrt{\pi}}\int_0^f df' \sum_{k=-\infty}^{\infty} \exp[-\beta^2(k+\alpha f')^2]. \tag{21}$$

The explicit calculation for the excitation rate reads

$$r_1^0(F) = \frac{v}{\ell}(1-f)\frac{1}{\alpha+\phi(f)}, \tag{22}$$

so the efficiency can then be expressed as

$$\eta_1^0(F) = \phi(f)\frac{F\ell}{\Delta\mu}. \tag{23}$$

An alternative expression for $\phi(f)$, which is convenient for the case of large β is

$$\phi(f) = \frac{1}{2}\Bigg[\operatorname{erfc}(\alpha\beta f) + \sum_{k=1}^{\infty}\{\operatorname{erfc}[\beta(k+\alpha f)] - \operatorname{erfc}[\beta(k-\alpha f)]\}\Bigg]. \tag{24}$$

In the weak-noise limit ($\beta \gg 1$), the velocity-force curve may thus be approximated for a nonvanishing force by taking $\phi(f) \simeq \frac{1}{2}\operatorname{erfc}(\alpha\beta f)$. In this limit we have

$$V_1^0(F) \simeq v(1-f)\frac{\operatorname{erfc}(\alpha\beta f)}{2\alpha + \operatorname{erfc}(\alpha\beta f)}, \tag{25}$$

$$\eta_1^0(F) \simeq \frac{1}{2}\operatorname{erfc}(\alpha\beta f)\frac{F\ell}{\Delta\mu}. \tag{26}$$

III. REPULSIVE INTERACTIONS

A. Enhanced cooperativity for excluded volume interactions

To study the cooperative effects of the N-body problem we start by considering the simplest case of a hard-core repulsive potential. For practical reasons it is customary to model a hard-core repulsion of range σ using a Lennard-Jones potential,

$$W(\xi) = 4\epsilon\left[\left(\frac{\sigma}{\xi}\right)^{12} - \left(\frac{\sigma}{\xi}\right)^{6}\right], \tag{27}$$

for $\xi < 2^{1/6}\sigma$ and zero, otherwise. A new dimensionless parameter

$$\bar{\sigma} \equiv \frac{\sigma}{\ell} \tag{28}$$

is introduced in the problem, which is the size of the motor relative to the track period. The parameter ϵ is an auxiliary parameter that must be chosen large enough to ensure that the interaction is effectively hard-core for $\xi < \sigma$.

For the fully asymmetric model ($a=0$) in Ref. [25] it was shown that enhanced cooperativity occurs for an arbitrary number of motors N, except for very narrow windows in which σ is commensurate with ℓ. Here, we report further evidence of this conclusion extending it to the case $a \neq 0$.

1. Mechanism of enhanced cooperativity

The basic explanation for enhanced cooperativity was already sketched in Ref. [25] and relies on the fact that the two-motor configurations endow the leading motor with an additional mechanism to advance to the next ratchet site which is not noise dependent. In fact, the trailing motor can push the leading one beyond the ratchet barrier when the former is sliding down the ratchet potential (state U_1) and the leading motor is in the diffusive state (U_2). This situation happens relatively often if the leading motor is sufficiently loaded since then the velocity difference between the loaded and the unloaded motors brings them quickly together. The fact that the motors are unequally loaded is thus crucial for this mechanism to take place (at $F=0$ the two motors become independent and there is no cooperative effect). The opposite crossed-state configuration, with the trailing motor in the diffusive state and the leading one in the deterministic state, contributes unfavorably with respect to MF, but the statistical weight of this configuration is usually not dominant. Enhanced cooperativity is thus expected to be quantitatively more pronounced whenever the noise mechanism is very inefficient for the leading motor to advance, while still sufficiently effective for the unloaded motor to do it. That is, when there is a big difference between the velocities of the free and the loaded motors. For $a=0$ the effect is most dramatic in the limit of small noise strength $\beta \gg 1$. In fact, even though the stall force is noise independent, from Eqs. (20) and (25) it is clear that an apparent stall force may be defined when the velocity-force curve crosses over to its fast decay. From the condition $\alpha\beta f \sim 1$ it follows that the apparent stall force for a single motor may be defined as $F_{ap} = \lambda(4D/\tau)^{1/2}$. For forces larger than that, the MF analysis predicts velocities that fall off as $(F_{ap}/F)\exp(-F/F_{ap})$. Note that the velocity of the trailing motor and the contribution of its push on the leading one are deterministic, which are of order 1 with respect to noise strength, $\mathcal{O}(D^0)$, while the leading motor velocity is of $\mathcal{O}(\sqrt{D}\exp[-1/\sqrt{D}])$. Therefore, the ratio of the cluster velocity to the MF velocity goes to infinity in the limit of vanishing noise. For a finite asymmetry of the ratchet potential, $a \neq 0$, even though the ratchet effect becomes ineffective for weak noise, the enhancement of cooperativity is even more dramatic, in relative terms. The picture is the same for decreasing noise up to $\sqrt{D\tau} \sim a$, that is, when the typical diffusive length in the U_2 state is comparable to a, and the trailing, unloaded motor can still advance with a significant velocity. For even weaker noise, the ratchet effect becomes ineffective but the velocity of the motor pair remains necessarily on the order of the velocity of the single motor at zero force, at least for a range of small forces. The single-motor velocity at zero force now decreases to zero but not as fast as the single-motor velocity at finite force.

In Fig. 2 we plot some typical cases where moderate enhanced cooperativity can be visualized, in particular including cases with $a \neq 0$ (more dramatic examples can be found in Ref. [25]). A measure of the relative enhancement of cooperativity at a given force is expressed by the ratio

$$R_2(F) \equiv \frac{V_2(2F)}{V_2^{MF}(2F)} = \frac{V_2(2F)}{V_1(F)}. \tag{29}$$

For $\beta \gg 1$ we have, for $a=0$,

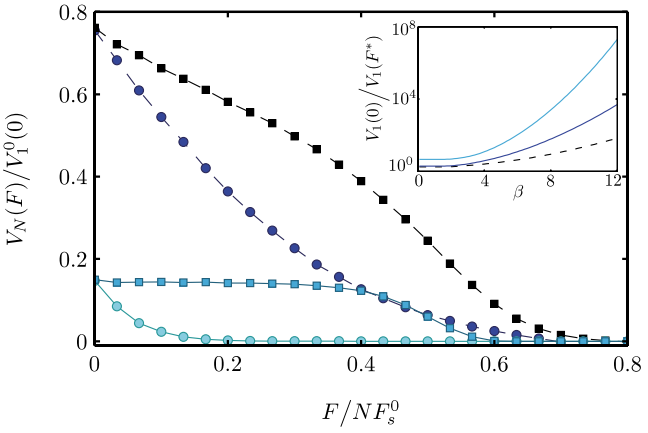

FIG. 2. (Color online) Velocity-force curves for $N=1$ (circles) and $N=2$ (squares) with hard-core interactions. Curves for $N=1$ coincide with the MF approximation of $N=2$. For all curves $\alpha=1/2$, $\bar{a}=1/10$, and $\bar{\sigma}=7/40$. Lower pair of curves (solid lines): $\beta=12.65$; higher pair (dashed lines): $\beta=4$. Normalization values $V_1^0(0)$ and F_s^0 are obtained from Eqs. (A5) and (A8). Inset: logarithmic dependence with β of the ratio between velocity at zero load and the velocity at $F^*=\frac{1}{3}F_s$ for a single motor. Each line corresponds to a different value of $\bar{a}$ (dashed line: $\bar{a}=0$). In all cases, $\alpha=1/2$.

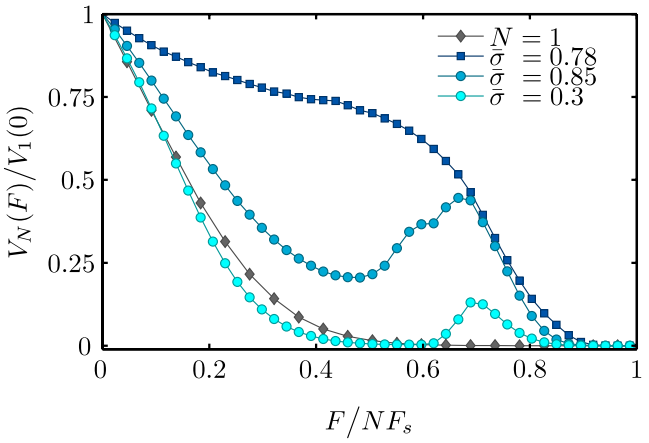

FIG. 3. (Color online) Nonmonotonic velocity-force curves with purely excluded volume repulsion with different values of $\bar{\sigma}$, for the minimal model; $\alpha=0.75$, $\beta=6.3$, and $\bar{a}=0$.

$$R_2(F) \sim \frac{V_1^0(0)}{V_1(F)} \sim \frac{2\beta\alpha^2 f\sqrt{\pi}}{(1+2\alpha)(1-f)} e^{(\beta\alpha f)^2}, \tag{30}$$

and for finite a,

$$R_2(F) \sim \frac{V_1(0)}{V_1(F)} \sim \frac{2\beta\alpha^2 f\sqrt{\pi}(1-\bar{a})\left[1+\bar{a}\left(\frac{1-\alpha f}{\alpha f}\right)\right]}{(1+2\alpha)(1-f)} \times e^{(\beta\alpha f\{1+\bar{a}[(1-\alpha f)/\alpha f]\})^2}, \tag{31}$$

in both cases diverging in the weak-noise limit. In the above expressions we have assumed that the numerators remain on the order of $V_1(0)$ in the weak-noise limit. This is found in the simulations and is the nontrivial point to ensure in order to prove rigorously the phenomenon of enhanced cooperativity in the weak-noise limit (see Sec. III B). The above ratios are plotted in the inset of Fig. 2, illustrating that the enhancement of cooperativity diverges even more strongly for finite a. We may thus conclude that the more inefficient the single motor performance is, the more enhanced is the motor cooperativity. Similar ratios can be defined for the efficiency. In fact, single motors become less effective when noise is weak and/or when the asymmetry of the ratchet is less pronounced. Changes in both directions imply that the motors tend to benefit most from motor-motor interaction.

2. Mechanism of reduced cooperativity

In Ref. [25] it was found that enhanced cooperativity was generic and essentially independent of σ except for a very narrow range of σ. For the two-motor problem, the most unfavorable situation was when $\sigma \simeq \ell$. The reason why this case leads to a degree of cooperativity that is worse than MF (reduced cooperativity) can be understood in simple terms. One must first realize that when two motors are in contact and in the same state, they do behave exactly as MF (the velocity is that of a single motor with $F/2$). If $\sigma=\ell$ the two motors would follow the same path synchronously except for fluctuations introduced by noise. Consider now the simultaneous excitation of the two motors to the U_2 state. The presence of a certain amount of noise implies an entropic repulsion that will force the leading motor to step forward in the next site, while the trailing motor will step backward. The motors will then loose contact for a finite time until they meet again. During this time, the velocity of the leading motor is smaller than the MF prediction. On the other hand, note that the pushing mechanism that explains enhanced cooperativity is less effective owing to the relatively high probability of the trailing motor to be pushed back by noise when it is at the high part of the potential U_1. Note that, in the above mechanism of reduced cooperativity, noise plays an essential role. By increasing the noise strength, the narrow dips in the velocity-σ plateau get wider and less pronounced. In Sec. VI we will give examples (see also Ref. [25]) and will also show that introducing a finite a has a similar effect than increasing the noise strength.

The above commensurability effect may be present as a reduction in cooperativity without necessarily implying a performance below the neutral cooperativity of MF. For instance, for a given motor cluster, changing the mean motor separation may be sensitive in regions where there is such commensurability. An interesting example is the possible appearance of nonmonotonic velocity-force curves even for purely repulsive interactions, as shown in Fig. 3. In those examples, for small forces commensurability leads to ineffective cooperativity, while increasing the force causes the two motors to become closer to each other and abandon the region of commensurability. In this case the effect is strong enough to actually increase the joint velocity. We see that in an intermediate range of forces, the behavior changes from almost MF to high cooperativity, as the external load is increased. Nonmonotonic velocity-force curves associated to the effect of the external force on the mean motor separation were reported for the case of attractive interactions in Ref.

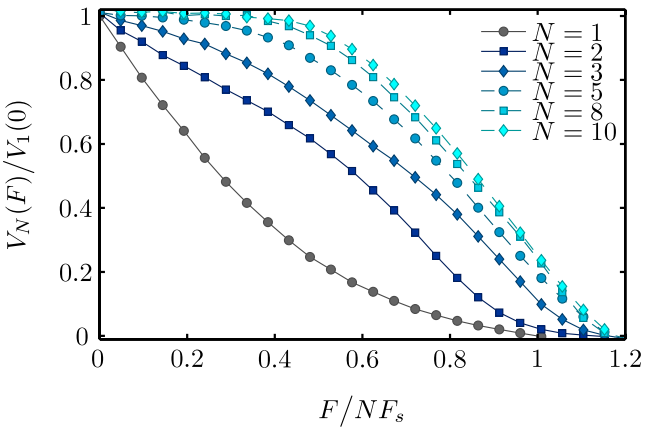

FIG. 4. (Color online) Convergence of the velocity-force curves with the number of motors N for hard-core interactions. For all curves, $\alpha=1/2$, $\beta=4$, $\bar{a}=1/10$, and $\bar{\sigma}=7/40$. Cooperativity is enhanced with an increasing number of motors until it saturates.

[25] and will be discussed for attractive forces in Sec. IV B. The above result illustrates the complex dynamical interplay between the motor size and the external force, which is most clearly manifest in the vanishing-noise limit (see Sec. III B and Ref. [39]).

3. Convergence with N and force transmission

Enhancement of cooperativity persists for increasing N. Typically it keeps increasing but with a weaker dependence on N for larger numbers of motors. In Fig. 4 we show a typical case, where the velocity-force curve exhibits a uniform and monotonic convergence with N to a limiting curve. A more remarkable case is shown in Fig. 5. This corresponds to the particular case in which σ is chosen in the very narrow range where the two-motor problem exhibits reduced cooperativity. Remarkably, even in this exceptional most unfavorable case, adding more motors contributes again to enhance cooperativity, emphasizing the really exceptional nature of the case with reduced cooperativity.

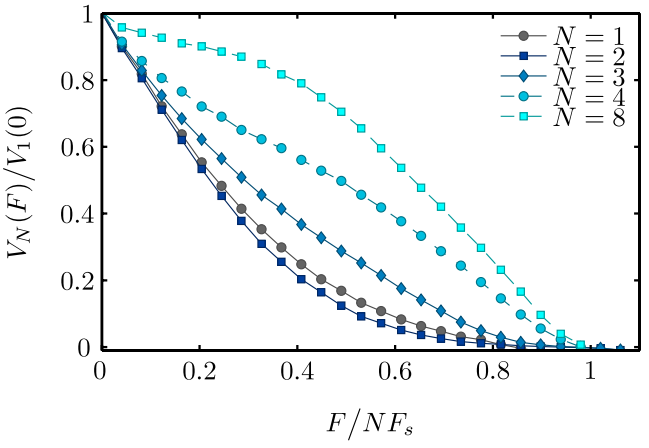

FIG. 5. (Color online) Velocity-force curves showing reduced cooperativity for $N=2$ but then progressively enhanced cooperativity for increasing N; $\alpha=1/2$, $\beta=4$, $\bar{a}=1/10$, and $\bar{\sigma}=7/10$.

The convergence for large N was discussed in Ref. [25] for the case $a=0$. An important conclusion was that the limiting curve for large N is a limiting function of F/N, implying that the force becomes extensive with the number of motors, in contrast to the result obtained by the discrete model of Ref. [17] where, for any finite force, the velocity-force was shown to converge to a function of F instead of F/N. The extensivity of the force reflects the existence of direct force transmission between motors and is a relevant point to assess in any model with large numbers of motors pulling on soft cargoes. It was assumed, for instance, in the simulations of [18]. For finite a, the large-N asymptotic may be more subtle, as new nontrivial phenomena take place (see Sec. VII).

B. Proof of enhanced cooperativity: Exact results for the two-motor problem

Since the mechanism of enhanced cooperativity is of deterministic origin, it makes sense to pursue an analytical understanding of our model in the weak-noise limit. This can be done all the way to $D=0^+$ in the fully asymmetric case $a=0$ (we assume the limit $\beta\bar{a}\to 0$ taken before $\beta\to\infty$), in which a single motor has still a finite velocity at zero force. In this limit we can rigorously prove the existence of enhanced cooperativity in some parameter regimes.

We first address the inexistence of reduced cooperativity in the above limit by proving the inequality

$$V_N(F) \geq V_1(F/N), \tag{32}$$

which is a weaker condition than Eq. (14). Since in the weak-noise limit $V_1(F)=0$ for any finite F, then it suffices to proof the non-negativity of the cluster velocity. A necessary condition of non-negative velocity of a single motor is obviously $F\leq\lambda v$. On the other hand, it is also necessary that $F\tau/\lambda<\ell$, so that when receding in the U_2 state it does not reach the ratchet period behind. Therefore, a sufficient condition for the velocity of a single motor to be non-negative for the full range of forces $0\leq f\leq 1$ is $\alpha\leq 1$. This result can be generalized to clusters of N motors, for which the sufficient condition for non-negative velocity is again $\alpha\leq 1$ for the full range $0\leq f\leq N$. The proof is simple if one avoids possible effects of commensurability, so the conclusion holds at least for all irrational values of σ/ℓ.

In order to prove the actual occurrence of enhanced cooperativity [the strict inequality $V_N(F)>V_1(F/N)$] for $D=0^+$ it suffices to show that $V_N(F)>0$ for finite F. This is not so simple in general, but it is possible to find parameter ranges where this can be easily done. The conclusion, however, is claimed to be valid in much broader ranges of parameters than those for which a simple proof is available. In Appendix B we sketch the proof that, for $N=2$, the simple condition

$$\frac{1}{8}\alpha<\frac{\sigma}{\ell}<1-\alpha \tag{33}$$

is a sufficient condition for enhanced cooperativity for the whole range of forces $0<f\leq 1$. Although this condition holds for relatively small values of α, enhanced cooperativity is also found for larger values of this parameter. A particular

TABLE I. Table of exact values for the two-motor velocity for the case $\alpha=1$, $\bar{\sigma}=1/3$ in the limit $D=0^+$ for a particular set of values of force. Note that the dependence is nonmonotonic, reflecting the complex geometry of the actual limiting curve, with a large number of discontinuities and fractal structure, as discussed elsewhere [39].

f	0	$\frac{1}{4}$	$\frac{1}{3}$	$\frac{1}{2}$	$\frac{2}{3}$	$\frac{5}{6}$	1
$\frac{V_2}{v}$	$\frac{1}{3}$	$\frac{21}{86}$	$\frac{35}{131}$	$\frac{81}{308}$	$\frac{28}{117}$	$\frac{35}{156}$	$\frac{1}{6}$

case that can be easily calculated for arbitrary N and α is that of the force $F^*=(N-1)\lambda v$, for which we obtain exactly

$$V_N(F^*)=\frac{v/N}{1+2\alpha}=\frac{1}{N}V_1(0)>0, \tag{34}$$

again with the exception of values of σ commensurated with ℓ. Remarkably, for $N=2$ it can be shown, with the help of graph theory, that $V_2(F)$ can be exactly determined in the limit of vanishing noise for any F in very broad parameter ranges. The calculation must be performed separately for each value of F, and it gives rise to rather complex geometrical properties of the velocity-force curve, including large number of discontinuities and fractal structure. For the present discussion it is relevant to stress that V_2 is positive (except possibly for windows of force with zero velocity). These results will be proven and discussed in detail elsewhere [39]. As illustrative examples of nontrivial exact solutions we report without proof several values of $V_2(f)$ for the case of $\alpha=1$ and $\sigma=\ell/3$ in Table I.

Similarly, in some parameter regimes it is possible to find relatively simple positive-defined lower bounds of $V_2(F)$ that prove enhanced cooperativity for a continuous range of forces. For instance, for $0<f<1$ and with the condition $\frac{1-f}{2}\alpha<\frac{\sigma}{\ell}$, it can be shown that [39]

$$V_2(f)>\frac{v(1-f)^2/4}{\sigma(3-2f)/l+\alpha(1-f)^2(4+f)}>0. \tag{35}$$

We conclude this section by emphasizing the remarkable fact that the joint velocity of the motor pair is finite for vanishing noise and against a finite external force. The system is thus able to perform a finite mechanical work by combining motors that are unable to produce any work at all at any finite force if taken separately. The fact that the combination of powerless motors is capable to produce a finite power in the limit of vanishing noise illustrates that another mechanism of directed motion, which is essentially deterministic, is at work. This mechanism, isolated here in the limit $D=0^+$, is at the root of the enhancement of cooperativity in the general case, where it coexists with the ordinary noise-driven ratchet mechanism. A similar phenomenon where directed motion is generated in the absence of noise in a two-state ratchet is known when motors are rigidly coupled. Nevertheless, we stress that in our case the motors have only excluded volume repulsion, that is, there is no attraction that can be invoked to form a motor assembly and to allow a leading motor to pull on a trailing one. The motor association here is purely dynamical, originating from the fact that the external force is asymmetrically applied.

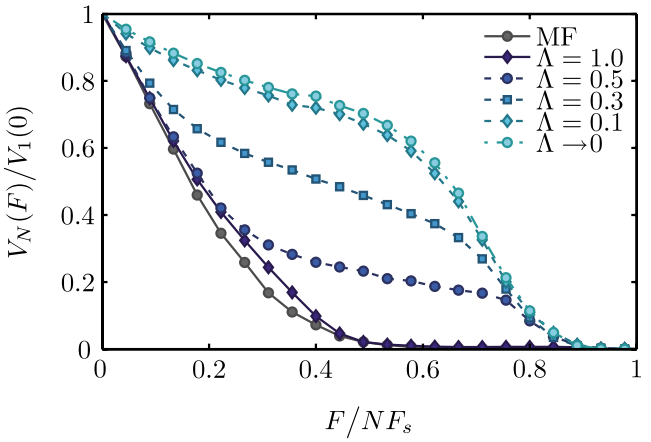

FIG. 6. (Color online) Convergence to mean-field behavior due to long-range interactions. An increase in the characteristic length of the long-range potential Λ destroys the enhanced cooperativity of the hard-core case, for small forces. See discussion of the crossover force in the text; $\alpha=2/3$, $\beta=6.68$, $\bar{a}=0$, and $\bar{\sigma}=0.2$.

C. Convergence to mean field

As it has been previously explained, the MF behavior can be obtained as a limiting case for sufficiently long-ranged repulsion or for sufficiently strong noise. We first address the convergence to MF when the range of the interaction potential is increased. We add an exponential tail of the form

$$W_L(\xi)=\kappa\Lambda e^{-\xi/\Lambda}, \tag{36}$$

for all ξ to our hard-core potential, where κ is the effective strength of the tail and Λ is its characteristic range of the repulsive interaction. In Fig. 6 we show the convergence to MF at fixed noise strength, in a case with sufficiently weak noise, so that for short-range interactions we have strong cooperativity. Notice that the convergence to MF is not uniform and occurs first for smaller forces, consistent with the criteria proposed in Sec. II C 2. The force F_{cross} at which the MF curve starts to cross over to the hard-core one can be obtained by a simple argument. As long as the repulsion is dominated by the exponential tail, the MF curve is supposed to hold. In the case of two motors, this covers forces for which $F/2$ is smaller than the maximal slope of the exponential tail (for $\xi<2^{1/6}\sigma$). Similarly, for arbitrary N we have $F_{cross}=-NW_L'(2^{1/6}\sigma)=N\kappa e^{-2^{1/6}\sigma/\Lambda}$. For larger forces the motors start to feel the hard-core and gradually enhance cooperativity until the hard-core result is reached.

Next we check the convergence to MF by increasing the noise strength while keeping the hard-core repulsion. Results are shown in Fig. 7 where we plot the relative deviation from MF behavior. In the limit of strong noise the deviation from MF tends to vanish. In this limit, the single-motor velocity-force curve and therefore the N-motor curve are linear and take the simple form

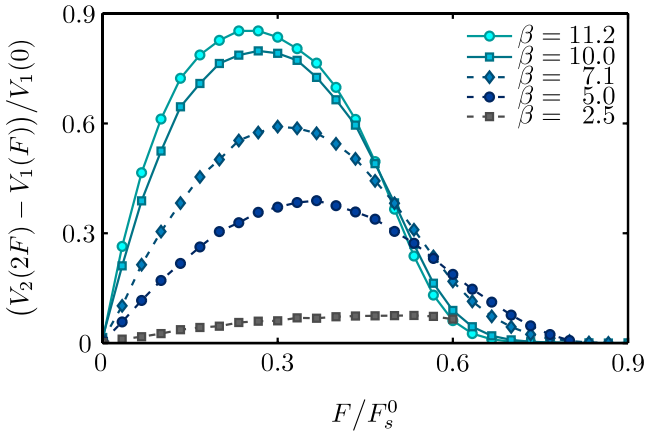

FIG. 7. (Color online) Cluster velocity decays to mean-field behavior for increasing noise strength (decreasing β); α=0.37, $\bar{a}$=0.1, and $\bar{\sigma}$=0.3.

$$V_N(F) = V_1(0)\left(1 - \frac{F}{NF_s}\right), \tag{37}$$

where F_s is the single-motor stall force. The above expression is a quite common assumption in many studies involving motor cooperativity. While this relation may be justified for rigid motor assemblies, for motors pulling on soft cargoes it is only achieved in the strong-noise regime.

IV. ATTRACTIVE INTERACTIONS

A. Strongly coupled motors

Although our main focus in this paper is on weakly coupled motors (nonbinding potentials), in the context of attractive interactions it is interesting to recall first the case of strong coupling, close to a rigid assembly of motors, a case that has already been studied extensively for similar models [9,40–42] and that is relevant to the subsequent discussion. To model a strong elastic coupling we use a harmonic potential of the form $W_S(\xi)=\frac{1}{2}k(\xi-\sigma)^2$, where k is sufficiently large. From the equilibrium relation $\langle(\xi-\sigma)^2\rangle_{\rm eq}=k_BT/k$ we choose k such that $\langle(\xi-\sigma)^2\rangle_{\rm eq}\ll\ell^2$ and express it in the dimensionless form

$$\bar{k} \equiv \frac{\langle(\xi-\sigma)^2\rangle_{\rm eq}}{\ell^2} = \frac{k_BT}{k\ell^2}, \tag{38}$$

which is an indicator of the relative deviations from the equilibrium position.

One of the known results of the rigid coupling case is that the velocity of a cluster at zero force is significantly higher than the one of a free motor. The cooperativity acts now in both ways, not only the motor behind pushes one ahead to the next period, but the one ahead also pulls on the trailing one. As long as motor separation and track periodicity are incommensurate, the velocity increase at zero load soon becomes independent on the number of motors and saturates. In Fig. 8 we summarize the qualitative scenario for a representative case.

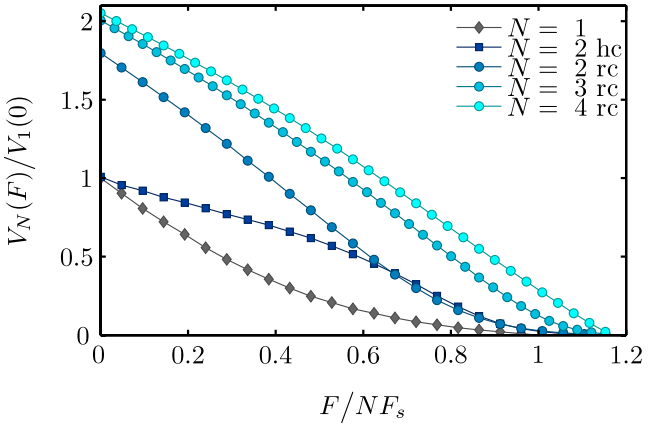

FIG. 8. (Color online) Velocity-force curves for rigid coupling (rc). Hard-core (hc) curve for two motors is also shown (squares). Although the free motor velocity now depends on the number of motors, it quickly saturates; α=0.5, β=4, $\bar{a}$=0.1, $\bar{\sigma}$=0.235, and $\bar{k}=10^{-4}$.

B. Weak attractive coupling

The weak attractive coupling between motors is introduced using the full Lennard-Jones potential (27). This potential is nonbinding in the sense that, with this interaction, the mean distance between two particles diverges, for any noise strength. Similarly, a particle can only be trapped transiently in the well and will escape from it to any distance in a finite time. Since we are interested in weakly attractive interactions, the depth of the well will be chosen so that the characteristic lifetime of a particle pair is relatively small. If the particles are motors of our ratchet model, this means that, at zero load, thermal fluctuations can break the motor cluster in relatively short time scales. In this way the spontaneous formation of a cluster is not attributed to the attraction but to the kinematic effect associated to the uneven distribution of the load, as before.

Under these circumstances, the joint velocity of a set of motors at zero load is the same as the free motor one, like in the hard-core case. As soon as the leading motor is subject to an external load, a stable cluster will form. The key difference with respect to the purely repulsive case is that now the leading motor can pull on the trailing motor while the former is sliding down the potential. To the extent that the cluster can be kept compact, the behavior will be reminiscent of that of a rigidly coupled assembly. Remarkably, the larger the external force the more compact and stable will become the cluster. Therefore, we may find that increasing the external load the joint velocity of the cluster does increase. This type of cooperative nonlinear response was first reported in Ref. [25] for the fully asymmetric case, a=0. This increase with the load must eventually be reversed for even larger forces, giving rise to a nonmonotonic behavior of the velocity-force curve. Here, we generalize this phenomenon to arbitrary a. A typical example is shown in Fig. 9.

The nonmonotonicity of the velocity-force curve is associated with a plethora of new dynamical phenomena. Contrary to all previous cases, now the number of motors in the cluster is not determined by the number of available motors,

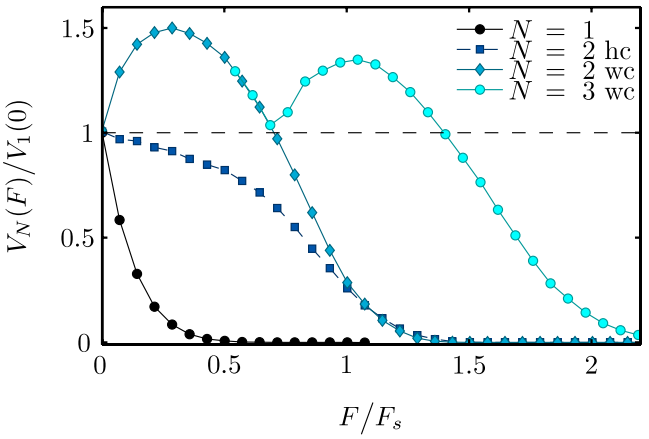

FIG. 9. (Color online) Velocity-force curves for weak attractive coupling (wc) and $N=2,3$ motors. Comparison with the hard-core (hc) case is also shown (squares). The horizontal dashed line indicates the maximum velocity of a single motor. The presence of an attractive force between the motors introduces a nonmonotonic behavior of the velocity-force relationship; $\alpha=0.18$, $\beta=14.1$, $\bar{a}=0.1$, and $\bar{\sigma}=0.2$.

but it is dynamically selected by the system. In particular, if we assume that there is an infinite reservoir of motors behind the cluster, no matter how large the load on the first motor is, it will keep recruiting motors up to the point where the motor cluster surpasses the velocity of a free motor. At that point the cluster will escape from the motor reservoir. This effect can be seen in Fig. 10. Similarly, if we progressively increase F, every time the cluster velocity decreases below the free motor velocity (dashed line) a new motor will be recruited if available. Upon increasing the force, the cluster velocity will

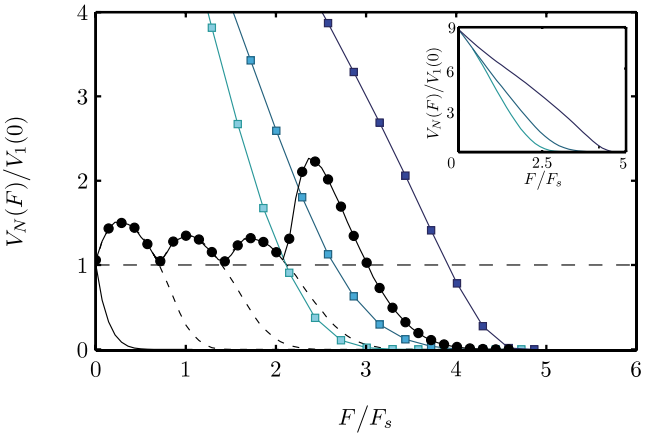

FIG. 10. (Color online) Velocity-force curve for weak interaction for $N=5$ motors (black dots) with the parameters of Fig. 9. Due to commensurability effects the cluster of five motors becomes highly compacted and can advance much faster than the four-motor cluster. Squares: velocity-force curve for a five-motor cluster bound with a rigid coupling for three values of the stiffness ($\bar{k}=10^{-4}$, 10^{-3}, 10^{-2} from left to right). We can clearly see that the behavior of the weak case approaches the one of rigid coupling. Also, on the rigid coupling, a smaller stiffness increases the overall cooperativity of the cluster. Inset: the full velocity-force curves for the rigid coupling (same three curves).

increase again until it reaches a maximum value and will decrease until the next recruitment. In the neighborhood of the points where the curve bounces up, hysteretic phenomena takes place in the form of a transient bimodality of the velocity distribution, as reported in [25], owing to the finite time that is required to recruit a new motor (for increasing F) or to release one from the cluster (for deceasing F). Remarkably, for any given external force, no matter how large it is, in the presence of a motor reservoir, the system will self-organize in a stable number of motors which will be actually advancing with a velocity that it larger or, at worse, equal to the free motor velocity (and therefore it will escape from the motor reservoir). The effect of a relatively small attraction between motors thus introduces a qualitative change in the dynamical scenario and implies an even more pronounced enhancement of motor cooperativity (see Sec. V below).

If, on the other hand, the number of available motors N is fixed, the curve of $V_N(F)$ coincides exactly with $V_2(F)$ for the first bump (the force range where cluster of more than two motors are metastable, and only the two-motor cluster is stable), with that of $V_3(F)$ for the second bump (the three-motor cluster is stable, and a two-motor cluster recruits a third motor) and similarly up to the $N-1$ bump. Only after that it decreases below the free motor velocity.

This type of bouncing velocity-force curves was first reported in Ref. [25] for the fully asymmetric ratchet $a=0$. In that case, the successive maxima of the curve followed a decreasing envelop. Remarkably, for finite a, additional phenomena come into play. As shown in Fig. 10, a sudden increase in some of the bumps may occur, due to commensurability effects between σ and ℓ, once a second length is introduced in the problem. In fact, when a multiple of the mean motor separation is close to a multiple of ℓ, the system becomes highly sensitive to being below or above this resonant condition. In the former case, the cluster is more compact since the motors in the extremes will typically lie at positions of the ratchet of opposite slope, implying a systematic compressive force that keeps the cluster more compact. Therefore, in that case the motor will be more cooperative. This is the case shown in Fig. 10. By slightly changing σ, one may reach the case in which the characteristic cluster size slightly exceeds a multiple of the ratchet period, implying the opposite effect, as one motor will become loosely associated to the cluster, thus implying a significant loss of cooperativity. In Fig. 11 we show how dramatically the rebound associated to the fifth motor completely disappears, while that of the fourth is significantly modified.

In Fig. 10 we also plot three curves corresponding to strong elastic coupling of motors for the case of five motors, for different degrees of rigidity of the harmonic interaction between motors. Notice that the actual curve is remarkably sensitive to the rigidity and gives actually more effective cooperativity for softer coupling. The curve of five motors with our weak coupling is bound by one of the softer harmonic couplings, but actually surpasses the case of the highest rigidity, indicating that a cluster with weak attractive interaction, when a sufficiently high load is applied, behaves as a compact group of mutually bound motors with a relatively loose elastic coupling. We also observe that a certain degree of fluctuations of the relative positions of motors in an oth-

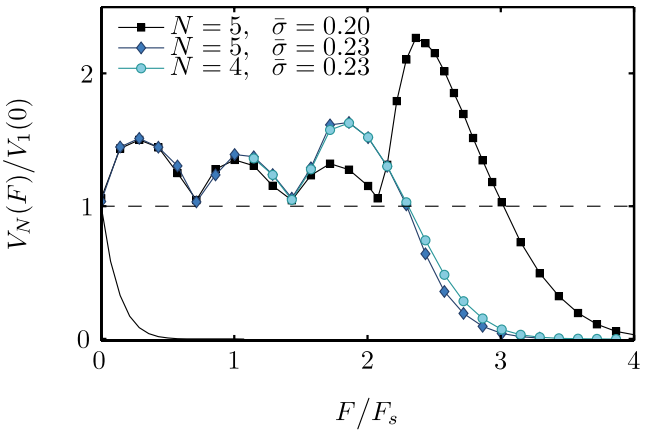

FIG. 11. (Color online) The same velocity-force curve from Fig. 10 (squares) compared with the same curve for a different $\bar{\sigma}$'s (diamonds). A small change in the motor size completely removes the effect of the last motor. Previously the recruitment of the fifth motor created a huge increase in velocity; now its recruitment has no impact on the velocity. Notice how the $N=4$ (circles) and $N=5$ (diamonds) curves are almost the same now. In this case (diamonds) due to commensurability effects the fifth motor never attaches to the other four. The minimum distance between the fifth and the first motors is such that the asymmetric part of the ratchet is continuously breaking the cluster.

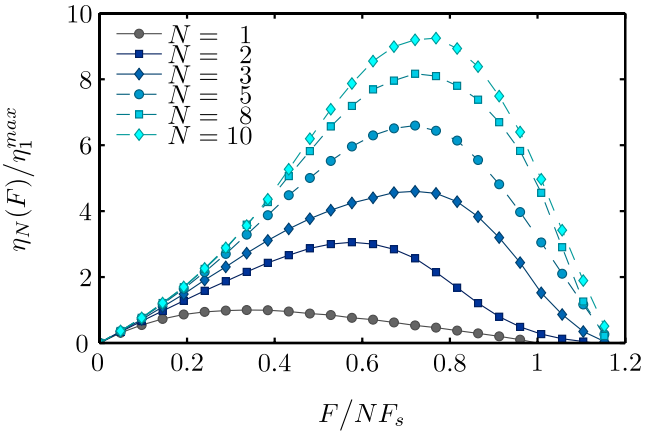

FIG. 12. (Color online) Efficiency curve for hard-core interactions. The efficiency of the cluster increases with the number of motors until it starts to saturate; $\alpha=1/2$, $\beta=4$, $\bar{a}=1/10$, and $\bar{\sigma}=7/40$.

erwise compact cluster does actually favor cooperativity (see also Sec. VII) and may outperform the case of strictly rigid coupling.

V. COLLECTIVE EFFICIENCY AND MOTOR COORDINATION

The collective efficiency is also an important quantity to characterize the cooperativity of motors and a convenient one to define the collective performance, as discussed in Sec. II C 3. We recall that, according to our definitions, the MF reference case corresponds to the condition $\eta_N^{MF}(F)=\eta_1(F/N)$. For short-range potentials and in the limit of weak noise, the relative enhancement of the cooperative efficiency with respect the MF prediction becomes arbitrarily large, on the basis of the asymptotic analysis of Sec. II D, since the single motor problem itself becomes very inefficient. Nevertheless, for moderate values of parameters a significant increase efficiency is found generically. Examples for $a=0$ were already reported in Ref. [25]. An example for $a\neq 0$ is shown in Fig. 12 for purely hard-core repulsion, where we normalize to the maximum of the single-motor efficiency curve $\eta_1^{\max}=\max[\eta_1(F)]$. The comparison with the curve $N=1$ gives directly the increase in efficiency with respect to MF.

In Ref. [25] it was also shown that, if a weak attractive interaction was added to the hard core, the increase in efficiency is even more pronounced. For $a\neq 0$ this is also the case but the situation becomes more complex due to commensurability phenomena such as those described in the preceding section and in Sec. VI (results not shown).

An upper bound of the efficiency at a given force can actually be determined that defines the theoretical limit to cooperativity within the two-state model at hand. In fact, if we consider a set of N motors with velocity V_N, the reaction rate has a lower bound of the form

$$r_N(NF) > r_N^{inf} = NV_N/\ell, \tag{39}$$

which corresponds to each motor requiring only one excitation to advance one period. This corresponds to an optimal limit in which the motors move in a highly coordinated mode. Consequently, an upper bound of the efficiency of N motors loaded by a force NF is given by

$$\eta_N(NF) < \eta_N^{sup}(NF) = \frac{F\ell}{\Delta\mu}, \tag{40}$$

which does not depend on N.

In general the efficiency increase combines an increase in the exerted power FV_N and a reduction in reaction rate. The latter is typically dominant and measures a certain increase in motor coordination, which in the case of large clusters involves a remarkable synchronization of the individual motors (see Sec. VII). The effect on the reaction rate can be seen in Figs. 13 and 14, where the rate per motor is plotted (parametrically on F) against velocity for weakly attracting interactions (with $a=0$) and hard core (with $a\neq 0$), respectively. For weak attraction, the curves in Fig. 13 refer to the range of velocities from the corresponding velocity-force curves of the type shown in Fig. 9 for weak attraction, all the way to zero (clusters with fixed N). All curves in Fig. 13 are qualitatively similar, but the overall decrease with the number of motors is remarkable. A significant difference between the $N=1$ case and the rest is the sign of the slope in the right end. For $N>1$ the rate per motor does decrease for increasing force (moving from right to left along the curve). This reflects the increase in coordination of the motor movements. For a single motor, instead, an increase in the force decreases the probability of stepping forward, and hence it decreases the velocity and increases the excitation rate. Note also that in the regime of large velocities, the curves for $N>1$ approach the asymptotic line of the theoretical minimum of the

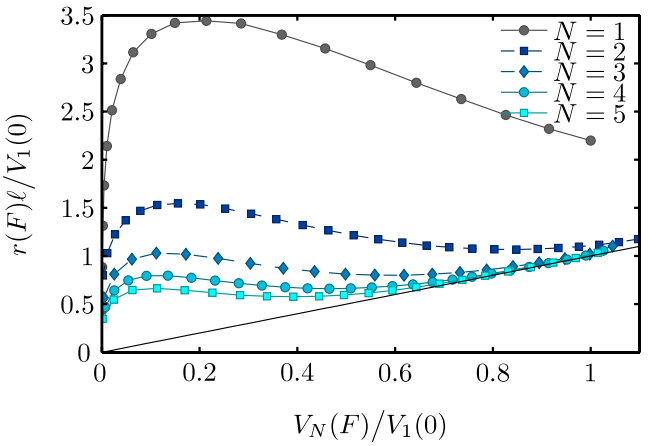

FIG. 13. (Color online) Excitation rate per motor $r(F)=r_N(F)/N$ along a complete velocity-force curve trajectory with weak attraction, for the fully asymmetric case. We can see a dramatic change in the rate with the introduction of more motors. The rate approaches its minimum value (given by the straight line) for high velocities; $\alpha=0.15$, $\beta=14.1$, $\bar{a}=0$, and $\bar{\sigma}=0.2$.

excitation (at a given velocity). Therefore, at maximal velocity the motion becomes optimally coordinated (one excitation, i.e., one ATP molecule, per step) and essentially ballistic.

For the case of purely hard-core repulsion, the situation is qualitatively different because the maximal velocity does not occur at finite but at zero force. This is the reason why the reaction rate per motor behaves differently in the extreme of high velocities. In any case, for the intermediate range of velocities and forces, the decrease in reaction rate per motor for increasing N is remarkable.

When we consider that behind the cluster there is a motor reservoir, as for the tube pulling experiments [21], the energetic efficiency behaves also qualitatively differently depending on whether or not a weak attraction is present. For purely repulsive interactions, the cluster velocity is bound by

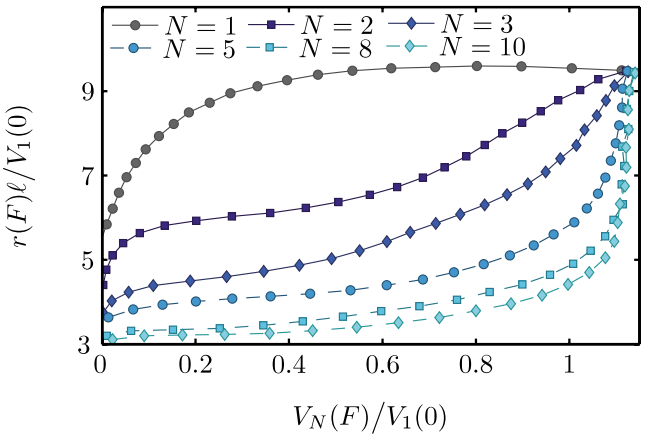

FIG. 14. (Color online) Excitation rate per motor for hard-core interaction and finite asymmetry. Although the rate does not approach its minimum value like in the fully asymmetric case, the strong reduction with the number of motors is still present; $\alpha=1/2$, $\beta=4$, $\bar{a}=1/10$, and $\bar{\sigma}=7/40$.

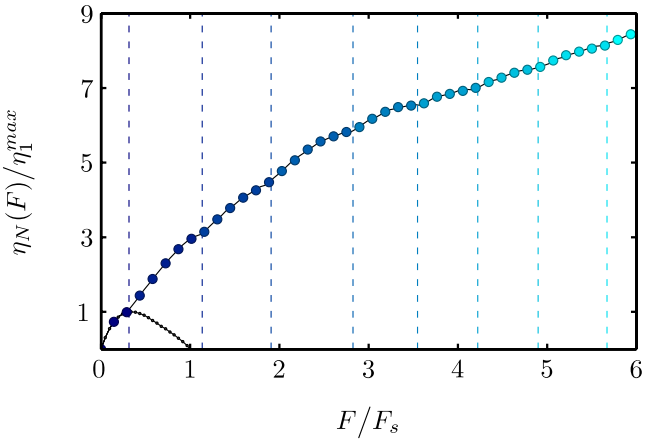

FIG. 15. (Color online) Maximum efficiency curve for hard-core interaction. The number of motors is chosen to assure maximal efficiency. Vertical dashed lines mark the addition of one motor to the cluster. The efficiency curve for a single motor is also shown (black line); $\alpha=1/2$, $\beta=4$, $\bar{a}=1/10$, and $\bar{\sigma}=7/40$.

the velocity at zero load $V_N(0)=V_1(0)$. Accordingly the motors behind the cluster will always catch up, so the number of motors in the cluster in not bound. For a fixed force F, the cluster velocity then tends to $V_1(0)$ and the total excitation rate diverges with N, implying a vanishing collective efficiency. However, in this case it is illustrative to consider the efficiency-force curve if we leave the number of motors as an adjustable parameter to maximize the efficiency at any given force. This yields the plot of Fig. 15, where the dashed vertical lines signal each addition of one motor to the cluster. Therefore, with the right choice of N, the efficiency-force curve is monotonically increasing and is potentially unbound, consistent with Eq. (40).

The situation is fundamentally different in the case of weakly attracting motors as a result of the scenario described in Sec. IV B. Since the cluster velocity typically surpasses the velocity of the unloaded motors for a sufficiently large N, the number of motors in the cluster is dynamically selected. Accordingly, this self-regulating mechanism does not maximize efficiency but the cluster velocity. Nevertheless, as argued above, the cluster achieves very large efficiencies precisely when the velocity exceeds the free-motor one, regardless of how large the force F is. This is remarkable, because in this arrangement each motor is moving at a velocity that is higher than that of the free motor and is nevertheless capable to generate a finite power, since the force per motor remains finite. Moreover, at the maximal velocity for a given N, condition (39) is satisfied, thus implying optimal coordination and ballistic motion, even with a reduced number of motors. In this optimal configuration, the motors push and pull the others in a coordinated way, so that each motor performs only one excitation at each site.

VI. EFFECTS OF COMMENSURABILITY

With any type of interaction, whenever a stable cluster is formed, resonance phenomena associated to the commensurability between the different length scales, ℓ, a and the

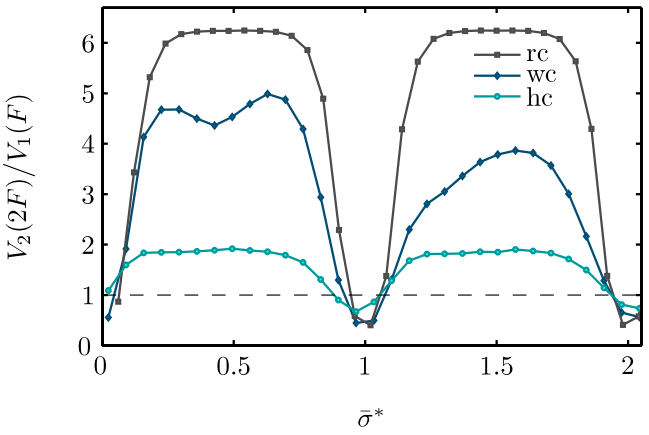

FIG. 16. (Color online) Velocity deviations with respect to mean field (dashed line) as a function of the effective motor separation $\bar{\sigma}^*$, for $N=2$ and the different interactions: squares for rigid coupling (rc), diamonds for weak attractive coupling (wc), and circles for hard core (hc). Commensurability effects are evident at $\bar{\sigma}^* \sim 1$; $\alpha=0.93$, $\beta=6.3$, $\bar{a}=0.1$, and $F=1/4F_s$.

mean distance between motors may have strong and nontrivial effects on the dynamics of the cluster. The mean motor-motor distance is controlled by the parameters of the interaction, but it also depends in general on the noise strength through some entropic repulsion between motors. For hard-core repulsion, the mean motor separation is slightly larger than σ and very weakly dependent on the position of the motor in the cluster (see an example in Fig. 18 of Sec. VII). The simplest example of such resonances is the mechanism of reduced cooperativity described in Sec. III A 2, taking place for $\sigma \simeq \ell$ in the case of hard-core repulsion. As proven in Sec. II D, this phenomenon requires the presence of noise. Increasing a has a similar effect than increasing noise strength in making the dips in the curve of velocity vs σ less steep and deep at the resonance. In Figs. 16 and 17, we compare this basic resonance in the cases of hard-core repulsion, weak attraction, and rigid coupling

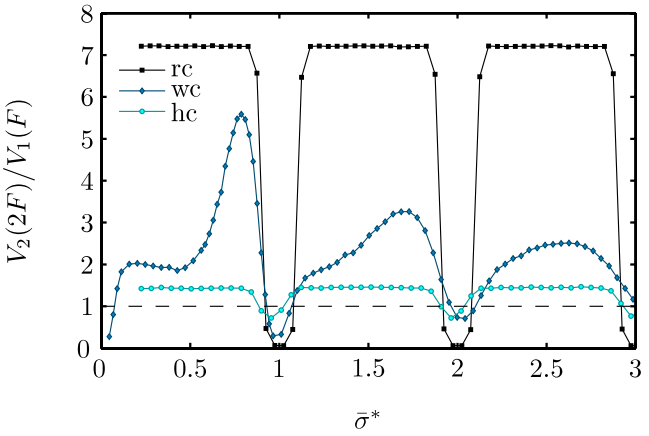

FIG. 17. (Color online) Same as Fig. 16, but with different parameters. Commensurability effects are still evident at $\bar{\sigma}^* \sim 1$. The asymmetric behavior of the curve for the weak interaction is due to different mean lifetimes of the cluster; $\alpha=0.18$, $\beta=14.1$, $\bar{a}=0.1$, and $F=1/10F_s$.

(strong elastic interaction, but not strictly rigid). We show the deviation from MF (the dashed horizontal line) as a function of the position of the minimum of the potential σ^* normalized by ℓ. The degree of cooperativity is increasing, respectively, and—except around the resonances—for the hard-core and the rigid coupling cases the curve is very flat, that is, independent of σ. For the rigid coupling case, the curve is periodic in σ by construction and the resonances are more sharp and pronounced. Changing σ in the Lennard-Jones potential, however, is not equivalent to a shift of the potential. In the truncated case (hard core, with $\sigma^*=2^{1/6}\sigma$), the curve remains nearly periodic, but in the weakly attractive the dependence on σ^* is clearly nonperiodic. Furthermore, it shows a secondary peak that is progressively smoothed out at successive periods of σ^*. This is a secondary resonance associated to the other length scale a.

For larger clusters, higher-order resonances whenever multiples of the mean motor separation are commensurate with multiples of the ratchet period will be possible and give rise to rather complex dynamical behavior. A remarkable effect of such resonances has been discussed in Sec. IV B to explain the results of Figs. 10 and 11, where a slight change in σ has a profound effect on the velocity-force curve when a condition of resonance is crossed. In this case it is required that $a \neq 0$. The presence of the steep part of the potential associated to finite a may have in general an strong impact on the inner structure of the cluster, and consequently on its dynamics, for instance, implying a rather uneven distribution of the average force supported by each motor in the cluster. This leads naturally to additional phenomena that may hinder cooperativity for large N, as briefly discussed in the next section.

VII. DYNAMICS OF LARGE CLUSTERS

A. Cluster structure, force distribution, and synchronization

Our modeling allows us to investigate the inner structure of the clusters, the force distribution among motors, and to what extent the motion of motors is coordinated into synchronous motion. We have seen that, with weakly attractive interactions, small clusters may exhibit highly coordinated motion. It turns out that for relatively large N, even with only hard-core repulsion, the clusters formed by applying a large force upon the first one become apparently rigid motor assemblies, with a roughly uniform mean separation close to σ. We may thus expect that the collective behavior must approach to some extent that of rigid coupling. In Fig. 18 we plot the spatial probability distribution of motors in a cluster for a representative example. The entropic repulsion is very small since noise is relatively weak, so the peak of the tenth motor is only slightly above $10\bar{\sigma}$. The width of the position peaks, however, is clearly dependent on the distance from the first motor, with only the last few being significantly spread. Under these conditions, the cluster structure is close to periodic and apparently quite rigid.

It is also interesting to investigate how the total force is distributed within the motors of a cluster. In studies of motor cooperativity it is customary to make the assumption that the motors have, on average, an equal share of the total force

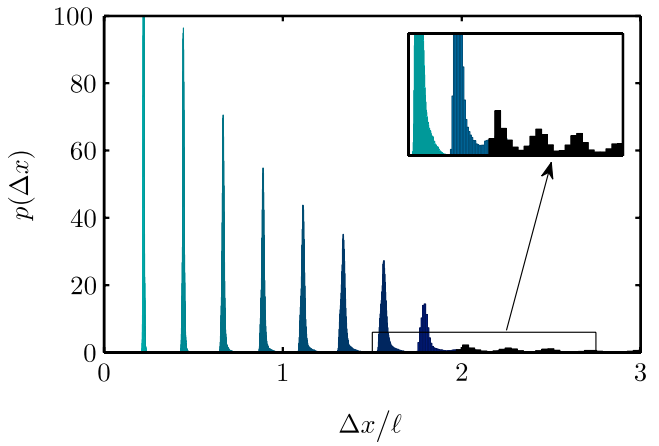

FIG. 18. (Color online) Probability density function for the relative positions of the motors ($\Delta x_i = x_1 - x_i$) inside a cluster with $N=10$ and hard-core interactions. Inset: zoom in on the last three-motor distributions; $F=N/2F_s$, $\alpha=0.18$, $\beta=14.1$, $\bar{\sigma}=0.2$, and $\bar{a}=0.1$.

F/N. This is relevant, for instance, to model the kinetics of motor binding or unbinding, which in general is sensitive to the applied force, as discussed in Ref. [18]. For the case of $a=0$, we show some representative results in Fig. 19. We find that, already for relatively small clusters, the time average of the total force acting on a given motor from the interaction with the other motors is indeed uniformly distributed among motors. The only exceptions are the very few motors at the end of the cluster in the case of repulsive interactions, since then the last motors are only loosely attached to the cluster. To the extent that the force distribution is uniform, the value must be close to the equal share prediction of MF, that is, F/N (slightly above for the case of repulsive interactions). Remarkably, this does not mean that the cluster velocity or efficiency is close to the MF prediction, since the values of the force do exhibit strong correlations, but suggests that for the kinetics of motor detachment the assumption of equal force share may be justified. For the general case of $a \neq 0$, however, the situation is much more complicated. An example of a small cluster is given in Fig. 20. Again, a slight change in σ produces a large effect of the resulting curve for $N=5$. The force distribution departs strongly from the uniform case in both situations, with two different qualitative shapes and with the total force of the extreme motors in the cluster changing considerably. It is also interesting to observe that the force distribution in the case of $N=4$ resembles very much that of $N=5$ with the larger value of σ, indicating that the reason behind this transition with σ is the same type of commensurability effect discussed in Fig. 11: the motor structure changes from a compact and rather rigid cluster of five motors to a less packed one of four motors plus a loosely attached one.

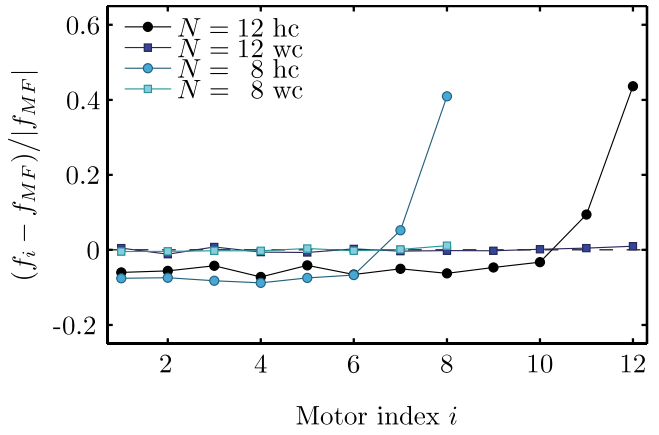

FIG. 19. (Color online) Force distribution along clusters of $N=8$ and 12 motors for $\bar{a}=0$ and $F=N/4F_s$. Circles are for hard-core interaction; the first six (ten) motors feel a force higher than the MF value, and the last two feel a much smaller force since they are not always attached to the cluster. Squares are for weak interaction; since the external force is strong, the cluster is stable and each motor shares almost the same load. Although not obvious from the force distribution, both clusters are highly cooperative. Other parameters: $\alpha=0.15$, $\beta=14.1$, and $\bar{\sigma}=0.2$.

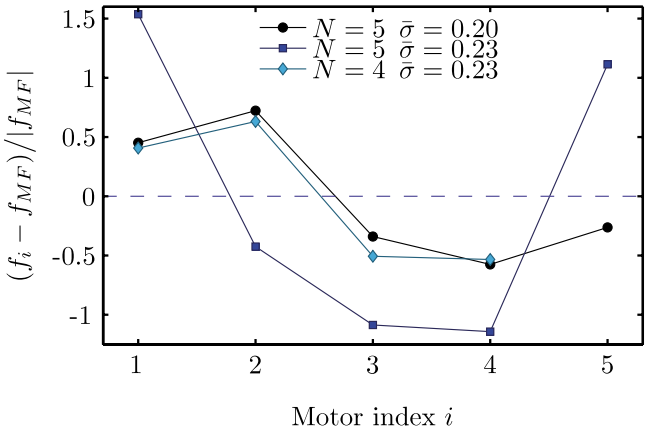

FIG. 20. (Color online) Force distribution for the different curves of Fig. 11 for $F/F_s=2.6$. Clear example of commensurability effects on the force distribution. A small change in the motor size (from circles to squares) creates a large qualitative change in the force distribution inside the cluster. Removing a motor (diamonds) moves the force distribution back to the previous form.

An important issue in modeling the dynamics of motor clusters is the degree of coordination of the motor steps in groups of motors. Different possibilities were investigated, for instance, in the problem of motors pulling on membrane tubes in Ref. [18]. In Sec. V we have addressed the issue of motor coordination of small clusters and have proposed a quantification in terms of the comparison with the theoretical minimum of the excitation rate. In addition to the coordination of the cycles of the motors (which one may associate to some degree of "frequency locking"), one may consider to what extent the stepping is synchronous ("phase locking"). For large N, the fact that the nearly periodic and rigid structure of the cluster is preserved implies that the stepping of motors is not only highly coordinated but highly synchronized. Typically, a large cluster will stay still until a sufficient number of motors can make a step and pull the whole cluster one step further. In Fig. 21 we show a characteristic trajectory of a motor cluster. Note that all motors except the last two move quite synchronously, even though the waiting time before each step is very stochastic. The motion is thus essentially nonperiodic but highly synchronized.

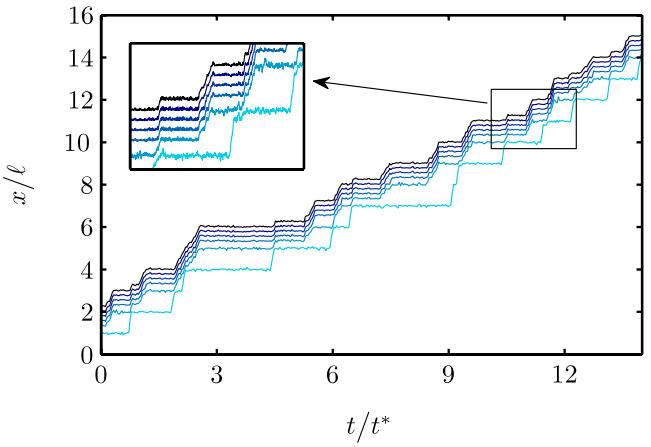

FIG. 21. (Color online) Trajectory for a cluster with $N=6$ and hard-core interaction; $t^*=\ell/V_N(F)$. Inset: zoom in on the trajectory; $F=N/2F_s$, $\alpha=0.18$, $\beta=14.1$, $\bar{\sigma}=0.2$, and $\bar{a}=0.1$.

B. Bidirectional motion

One interesting consequence of the highly compact and effectively rigid structure of large motor clusters, even if only excluded volume interactions are present, is that they will exhibit dynamical behavior of rigid motor assemblies with the same number of motors. One of the most striking features of these is the occurrence of bidirectional motion, that is, the existence of two possible velocities, one positive and one negative, and the occurrence of spontaneous transitions between the two. This stochastic bidirectional motion was described in Ref. [9]. Note that in both directions, the external force applied to the first motor tends to keep the cohesion of the cluster, so the cluster remains approximately rigid in both cases.

Figure 22 shows the trajectory of a motor cluster where bidirectionality is present. The two slopes of the trajectory clearly indicate two well-defined velocities. The velocity histogram can be seen in the inset. Finally, in Fig. 23 we illustrate how the presence of bistability manifests in the analysis of the velocity-force curve. We have plotted the continuation of the two velocity branches (the values of the two peaks of the bimodal velocity distribution) and the time-averaged curve that interpolates between them, when the spontaneous transitions between the two branches are averaged out. For very large N, the transition times become also very large, and the average curve in the limit of large N may be difficult to observe, as the system breaks ergodicity in that limit.

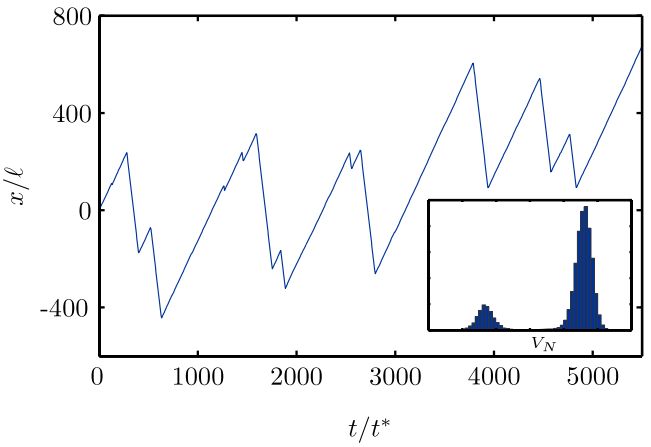

FIG. 22. (Color online) Trajectory of the mean position of a cluster of $N=40$ motors in the bimodality zone. The system clearly shows two different velocities that are maintained for long periods of time. $t^*=\ell/V_N(F)$. Inset: velocity distribution function showing the two peaks.

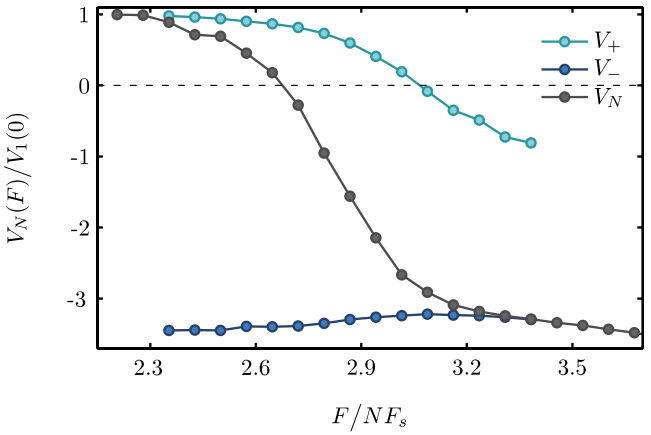

FIG. 23. (Color online) Velocity-force curve for $N=40$ showing the appearance of a second velocity peak and the sharp transition in the mean as the force is increased. V_+ and V_- represent the mean value of the velocity associated with each peak of the distribution, and V_N represents the global mean; $\alpha=1.85$, $\beta=1.9$, $\bar{a}=0.1$, and $\bar{\sigma}=0.37$.

VIII. IMPLICATIONS FOR BIOLOGICAL MOTORS

The key ingredient that brings out the type of motor cooperativity described here is the fact that an external load is applied to one or a few motors, while others are free to move unloaded until they meet the loaded ones. This situation is directly motivated by examples from the biological context. Under these circumstances a sort of "solidarity principle" makes the unloaded motors to team up with the loaded ones, not only to undertake the task jointly, but in general doing it more efficiently in group. In biological terms, the total mechanical work obtained per ATP molecule that is hydrolyzed is higher when motors act together. Similarly, the joint speed and the joint force are also enhanced beyond the simple superposition of the effects of individual motors. If, in addition, a certain degree of attraction between motors is present, the cooperative performance is further improved to the point where, for instance, each motor in the group contributes with a finite power while moving at a velocity that is higher than its velocity at zero load (situation in which it would perform no mechanical work). It remains an open question to elucidate to what extent biomolecular motors do take advantage of these possibilities for performing specific tasks.

It has now been recognized that several processive molecular motors do behave as Brownian motors, driven by a ratchet mechanism of noise rectification, most remarkably, the subfamily of monomeric kinesins called KIF1A and

KIF1B in mammals [30,43–45], together with their invertebrate counterpart, UNC104 [46], and also the MCAK motor that controls microtubule depolymerization [47]. The first two examples are found specifically in axonal trafficking, a situation where transport is most demanding due to the long distances traveled in axons and due to the particularly heavy trafficking conditions of them, with the possibility of traffic jams as a serious threat precluding neurodegenerative diseases such as Alzheimer's [32]. KIF1A is a monomeric kinesin motor specifically in charge of transport of synaptic vesicle precursors, an example of very large tubular vesicles (as long as 10 μm) [48] crucial for neuronal function, which have to be transported along the axon. It is rather puzzling that the most demanding transport requirements are assigned to relatively inefficient motors such as KIF1A, a noise-driven motor. Indeed, monomeric kinesin is not found in conventional intracellular traffic, where dimeric (two-headed) kinesin motors, which follow a hand-over-hand cycle, are not only more deterministic (nearly ballistic) but are also faster, stronger, and more efficient than the very noisy and erratic KIF1A. Our results in this paper suggest that the reason behind the specificity of KIF1A in transport of large soft cargoes along axons could be their high cooperativity in the arrangement of unequal loading. In large groups, which are required in axonal transport, monomeric kinesin may strongly outperform conventional kinesin. This refers not only to force transmission, velocity, and efficiency, but also to long-distance processivity, since the detachment kinetics from microtubules of KIF1A has also been claimed to be less sensitive to force than that for conventional kinesin [49]. One aspect of large motor clusters that does not have any obvious biological function is the bidirectional motion. Even though the actual cause is still unclear, it is worth mentioning that velocity reversal has actually been observed in axonal transport of large vesicles [48].

The above questions will be quantitatively explored in detail elsewhere [33], but it is worth completing the discussion here with some relevant numbers. The parameters of the two-state ratchet model adequate for KIF1A can be extracted from the literature [30,43]. The most determinant one is the noise strength which can be directly measured studying the diffusion in the weakly bound state. This yields values for D in the range $20-40$ nm^2 ms^{-1}, which indeed corresponds to the limit of large noise strength. During the lifetime $\tau \simeq 4$ ms of the weakly bound state, the typical diffusive displacement in that state is significantly larger than the ratchet period $\ell = 8$ nm. The strong-noise regime is the one that ensures maximal velocity of the single motor, with a linear velocity-force dependence, but gives the motor a strong randomness. This randomness is obviously rectified for large groups of motors in the presence of a strong force unequally loaded. The only approximation in our model that is not quite realistic for KIF1A is the vanishing dwell time assumed at the ATP-binding site (the lowest point of the sawtooth potential), which in the conditions of ATP saturation can be as large as 10 ms. This fact can be easily incorporated in our model but may have nontrivial effects in some cases. Preliminary simulations with realistic dwell times show that, for small and moderately large clusters, the extensivity condition is fulfilled for hard-core repulsion, so for this case and relatively small clusters, relation (37) holds. Finite processivity can also be incorporated following the scheme of Ref. [49]. When attractive interactions are included the dynamics is also highly cooperative but more complex [33].

While excluded volume repulsion can be easily justified and estimated for actual molecular motors, the origin of a possible weak attraction is less obvious. Attractive interactions of motor proteins in the kinesin superfamily have been explicitly reported in Ref. [50]. On the other hand, the possibility that monomeric kinesin motors are organized by lipid rafts in the membrane where they are linked [29,46,51] has been reported as a possible external mechanism of control of the cluster size, cohesion, and stability. This arrangement would introduce an effective attraction that could have similar effects to those reported in this paper for attractive interactions.

Concerning the most common family of dimeric kinesins, the present discussion is in principle not directly applicable because, even though there may be diffusive steps in the motor cycle, this is much more deterministic than monomeric kinesins. A more appropriate two-state ratchet model would not contain the diffusive weakly bound state, but two identical but shifted sawtooth potentials [26,49]. The interaction between motors is still an important element in the collective behavior of self-organized clusters pulling on fluidlike cargoes, but the possibility of direct force transmission seems probably more limited. In this case one may expect that the predictions of the ASEP approach of Ref. [17], implying a saturation of the velocity curves with the number of motors, could be more realistic than for monomeric kinesin.

IX. SUMMARY AND CONCLUSIONS

In this paper we have addressed the dynamics of groups of noise-driven processive motors that can be modeled by a two-state ratchet potential, when they are attached to a soft fluidlike cargo. This situation, motivated from real processes in cell biology, leads naturally to the prototypical problem where an external force is applied only to the leading motor and the rest accumulate behind. The asymmetric loading of the system is crucial for the formation of a motor cluster, and its dynamical behavior is nontrivially controlled by the value of the external force. This acts as an effective attraction that keeps the cluster dynamically stable and relatively compact, even though the direct motor-motor interactions are not capable to give rise to a true motor assembly. Therefore, one may call such motor clusters "self-organized." The effective attraction that holds the cluster together is from purely kinematic origin, since it results from the different velocity of the loaded and the unloaded motors. This in turn depends on the actual velocity-force curve of the motors, but the problem in general cannot be reduced to the knowledge of this characterization of the individual motor plus the mutual interactions. The nontrivial correlations between positional degrees of freedom and internal conformational states of motors due to mutual interactions result in a collective behavior that is genuinely different from that of the single motor problem. Some of the collective effects are reminiscent of phenomena already encountered in rigid motor assemblies, but other are

unique to the asymmetric loading of the system, typically those dependences on the external loading that originate from changes in the cluster inner structure and dynamics.

As a general conclusion, we have found that, generically, the joint performance of such self-organized clusters is better than the prediction of a mean-field ansatz that would imply the naive superposition of the individual contributions of the motors. The actual system outperforms the mean-field prediction in terms of force, velocity, and energetic efficiency. We have called this phenomenon "enhanced cooperativity." Within this scenario, whenever an external force is unevenly distributed to a set of motors, these team up to share the task of overcoming that force. Remarkably, with only repulsive interactions, this self-organized team work is such that each motor in the group will perform better than it would do if isolated and operating against its proportional part of the force. If, in addition, a certain degree of attraction is present between motors, then each motor contributes to the group much more than it would be capable of doing alone in any circumstances. For instance, it moves faster than alone in the absence of force, but performs mechanical work against a finite force.

We have shown that the mechanism of cooperativity is of deterministic nature and originates from the interactions between motors at different internal states. That is, a motor that is in the noise-driven state can be pushed (pulled) by another motor behind (ahead) that is sliding down the ratchet potential. In a situation where the noise is too weak, for the applied load to produce significant directed motion even if the load is split in half and half for two motors, under asymmetric loading a motor pair will be able to advance provided that the noise is sufficient to drive the unloaded motor. The trailing motor would catch up the loaded one and will push it forward whenever the right combination of respective states occurs. Note that in this example both the loaded and the unloaded motors make essentially no mechanical work (have zero efficiency) when separated, with one moving without external force and the other nearly stalling at a finite force. Similarly if the external load is equally distributed, the two motors would be nearly stalling. However, with asymmetric loading and simply hard-core repulsion, the motor pair will produce a finite power. This is possible, because once the motors interact, an additional mechanism of directed motion that is essentially noise independent is at work.

According to this analysis, the enhancement of cooperativity will be quantitatively more pronounced for small noise strength. If the ratchet potential of the motors is not fully asymmetrical ($a \neq 0$), there is a minimal amount of noise necessary for the deterministic mechanism to be effective. However, if we take the limit $a \to 0$ first, the cooperative mechanism of directed motion remains in the limit $D \to 0$. We have reported exact results for velocity-force and efficiency-force curves of the single-motor problem, and for the two-motor problem in the limit of vanishing noise. The former yield the asymptotic scaling of enhanced cooperativity in the limit of weak noise. The latter prove, in some ranges of parameters, that two motors with hard-core repulsion do have a finite velocity in the limit of vanishing noise. These analytical results rigorously prove the phenomenon of enhanced cooperativity in the weak-noise limit in some parameter regimes.

We have also studied the limits of long-ranged repulsive potentials and large noise strength to define the convergence to the mean-field behavior, a trivial situation which we may call neutral cooperativity. In this case, the cluster dynamics is in fact reduced to the single-motor problem. One important feature that is contained in this situation is the extensivity of the force, that is, the fact that the motors are able to transmit forces and therefore have an equal share of it. The phenomenon of force transmission, which is also present for enhanced cooperativity, is a natural consequence of the two-state ratchet model, but is a nontrivial result. In fact, for other approaches to cooperative motors under asymmetric loading, the possibility of force transmission is precluded or limited to relatively small numbers of motors [17].

The reversed phenomenon, which we called reduced cooperativity, has also been detected and analyzed. It has been shown that it occurs much more rarely, and typically it originates at particular parameter values that exhibit some kind of resonance. It also requires a significant amount of noise and is also more pronounced for less asymmetric ratchets. In any case, the phenomenon is quantitatively small and never as dramatic as its opposite phenomenon of enhanced cooperativity.

In the case where a weak (nonbinding) attractive interaction is added to the excluded volume repulsion the problem is dynamically richer. Nonmonotonic velocity-force curves with a rather complex structure are found. These lead to a self-regulation of the number of motors in the cluster into arrangements that have velocities larger than that of the unloaded motor and are performing a finite power per motor. The collective efficiency of these clusters is even larger than that for purely hard-core repulsion. In the conditions of maximal velocity (at any of the local maxima of the velocity-force curve), the motion of the motors becomes highly coordinated and approaches the theoretical limit of one excitation per step for each motor.

Nonmonotonic velocity-force curves have been reported in the literature in rather different contexts, in particular as a collective result of large numbers of strongly coupled motors, associated to the phenomenon of negative friction [8–10,52]. The mechanism responsible for this phenomenon here is completely different. It originates from the fact that changing the external force, the dynamical conditions leading to the formation of the cluster are modified. The statistics of the cluster structure, for instance, the average motor separation, are sensitive to the external force and at the same time are responsible for the degree of cooperativity. Accordingly, increasing the force may result in a more compact cluster, and hence a more cooperative one. This phenomenon is not exclusive of the attractive case. We have also shown examples for the case of pure hard-core repulsion.

Further nontrivial effects originate from spatial resonances when the motor separation and the scales of the ratchet potential show some degree of commensurability. The problem is particularly rich for finite asymmetry of the ratchet potential $a \neq 0$. Interesting examples where such resonance phenomena occur are exhibited, for instance, in the velocity-force curves of the case with weak attractive forces, where a rather nontrivial structure of the local peaks of the velocity-force curves has been elucidated.

The spatial structure of force transmission along the motor cluster has also been studied, showing a rather uniform force distribution for $a=0$, in particular for weak attractive interactions. For $a\neq 0$, however, the force distribution is in general highly nontrivial and sensitive to parameters. In particular, commensurability effects show also a rich scenario of qualitative force distributions.

Some of the most interesting collective effects emerge in the limit of large numbers of motors, with highly coordinated and nontrivial modes of propagation, such as the occurrence of bidirectional motion with spontaneous transitions between the peaks of a bimodal velocity distribution. Some of these phenomena are reminiscent of the dynamics of large rigid motor assemblies due to the fact that, in that limit, the motor cluster structure becomes very regular and periodic, thus effectively behaving as rather rigid assemblies. We have also shown that such clusters do behave quite synchronously even for purely hard-core repulsion.

Finally, we have briefly discussed the implications of the above results for actual molecular motors in biology. While it is yet unclear to what extent all these phenomena may actually be exploited in real biological processes, we have argued that, in general, the high cooperativity of Brownian motors pulling on soft cargoes could be a key ingredient to understand the role of monomeric kinesin motors in axonal transport, a problem of direct relevance to neurodegenerative diseases [32]. The specificity of these motors, which are highly inefficient when working individually compared to conventional kinesin, precisely for situations where the intracellular transport is particularly demanding, such as in axons, could be explained on the basis of their high degree of cooperativity when acting collectively. Nevertheless, regardless of the uses that biology may have developed of the possibilities of high collective performance of Brownian motors, these may always be potentially exploited in artificial motor setups, such as that of Ref. [53], which could potentially benefit from them.

ACKNOWLEDGMENTS

Financial support from Project No. FIS2006-03525 (Ministerio de Ciencia y Tecnología, Spain) is acknowledged. We are grateful to Otger Campàs and Jean-François Joanny for illuminating discussions.

APPENDIX A: EXACT SOLUTION OF THE SINGLE-MOTOR PROBLEM

Here, we sketch the exact calculation of the velocity-force curve for a single motor within the minimal model of Sec. II A. To simplify the calculation, the model assumes that the decay time from the weakly bound state U_2 is a constant τ and that noise may be neglected in the U_1 state. The dwell time at the minimum of the U_1 state prior to excitation is also neglected. None of these assumptions are crucial, and they may be relaxed without problem, but give rise to more complicated expressions.

Under these conditions, the only source of stochasticity is the diffusion in the U_2 state. The probability distribution for the position of the motor after the time τ with respect to the origin of coordinates at the initial position at one minimum of U_1 is simply

$$P(x)=\frac{1}{\sqrt{4\pi D\tau}}e^{-(x+F\tau/\lambda)^2/4D\tau}, \tag{A1}$$

where F is the external force, λ is the friction coefficient, and $F\tau/\lambda$ is the mean position. The motor will decay at $U_1(x)$ with the above probability distribution, and then slide down deterministically until a minimum of U_1 is reached, closing a cycle. This minimum can be the initial condition or belong to another period of the ratchet, thus implying a net displacement. The motion of the motor can be understood as a sequence of such cycles. On each cycle the motor is displacing a distance Δx that is by definition a multiple of ℓ and is spending some time that depends on the decay point x. If $\langle\Delta x\rangle$ is the mean displacement on a cycle and $\langle\Delta t\rangle$ is the average duration of the cycle, then the mean velocity is given by

$$V_1=\frac{\langle\Delta x\rangle}{\langle\Delta t\rangle}. \tag{A2}$$

Both numerator and denominator of this expression can be written explicitly using Eq. (A1). We have

$$\langle\Delta x\rangle=\sum_{n=-\infty}^{\infty}nl\int_{a+l(n-1)}^{a+ln}P(x)dx, \tag{A3}$$

$$\langle\Delta t\rangle=\sum_{n=-\infty}^{\infty}\int_{a-l+nl}^{nl}\left(\tau+\frac{-x}{v-F/\lambda}\right)P(x)dx+\int_{nl}^{a+nl}\left(\tau+\frac{x}{\frac{(l-a)v}{a}+F/\lambda}\right)P(x)dx. \tag{A4}$$

After some algebra the velocity may be expressed in the form

$$V_1(f)=v(1-f)\frac{\phi}{\alpha(1-\bar{a})+\phi+H}, \tag{A5}$$

where the function ϕ is given by

$$\phi=\sum_{n=-\infty}^{\infty}\int_{\bar{a}-1}^{\bar{a}}\frac{n\beta}{\sqrt{\pi}}e^{-\{[z+n+f\alpha(1-\bar{a})]\beta\}^2}dz, \tag{A6}$$

and H is given by

$$H=\sum_{n=-\infty}^{\infty}\int_{0}^{\bar{a}}\frac{z\beta e^{-\{[z+n+f\alpha(1-\bar{a})]\beta\}^2}}{\sqrt{\pi}(\bar{a}f+1-\bar{a})}dz. \tag{A7}$$

The stall force F_s can be directly obtained from these curves or from simple arguments. First, it must satisfy $F_s\leq\lambda v$ because no positive velocity is possible if the motor cannot slide down the ratchet potential. On the other hand, the mean velocity will be zero if, once in the U_2 state, the force brings the motor back to exactly the midpoint of the ratchet period at time τ. Therefore, the stall force is given by

$$F_s = \lambda v \min\left[1, \frac{1-2\bar{a}}{2\alpha(1-\bar{a})}\right]. \tag{A8}$$

Note that the above result is independent of noise because we have neglected diffusion in the U_1 state, thus preventing the possibility of the motor to go uphill in the ratchet potential. The result takes also a particularly simple form because of the condition of constant decay time τ, but the result can be easily extended to a distributed decay time.

APPENDIX B: PROOF OF ENHANCED COOPERATIVITY IN SOME SIMPLE CASES

Enhanced cooperativity is shown to be generic with only relatively small ranges of parameters where it is contradicted. Here, we sketch the proofs of enhanced cooperativity for $N=2$ in the limit of vanishing noise strength, in situations where this can be rigorously proved with rather simple arguments.

To proof enhanced cooperativity $V_N(F) > V_1(F/N)$ for $D=0^+$ we only need to show that $V_N(F) > 0$ for finite F because $V_1(F) \to 0$ for finite F. For $N=2$ if the motors can never go backward in the ratchet more than one period, we only need to show that there is a finite probability that both motors will advance to the next ratchet period. This can be easily proven if the two conditions of Fig. 24 are met.

Considering an initial condition in which the two motors are in contact at the bottom of state U_1, a first condition C1 requires that when the leading motor (the one loaded with the external force F) jumps to the weakly bound state U_2, it advances when pushed by the trailing one and falls after the decay time τ to the state U_1 before the second motor has reached the minimum of U_1. This can be expressed as

$$\tfrac{1}{2}(v - F)\tau < \sigma, \tag{B1}$$

where v is the sliding velocity and σ. In the dimensionless form this can be written as

$$\tfrac{1}{2}(1-f)\alpha < \bar{\sigma}. \tag{B2}$$

A second condition C2 requires that after the first motor has advanced a period due to C1 it cannot interfere in the possibility of the second motor to advance. Since the first motor can only move backward in the weakly bound state, this condition reads

$$\alpha f < 1 - \bar{\sigma}. \tag{B3}$$

Whenever both conditions C1 and C2 are met, we have proven that there exists a finite probability that both motors in the cluster advance to the next period. The motors will close the cycle by returning to the initial condition at the bottom of the state U_1 but in the next period of the ratchet potential. Now, combining both conditions we get a sufficient condition for enhanced cooperativity of the form

$$\alpha - 2\bar{\sigma} < \alpha f < 1 - \bar{\sigma}. \tag{B4}$$

From this result we may find a condition for the parameters that satisfies enhanced cooperativity for the whole range of forces smaller than the stall force, $f \in [0,1]$, which reads

$$\tfrac{1}{2}\alpha < \bar{\sigma} < 1 - \alpha. \tag{B5}$$

If we relax condition C1 to a less restrictive one, we can obtain a more general expression: when the first motor jumps to the weakly bound state, we may allow the second one to reach the transition point and change state. Now, with both motors in U_2 and moving backward due to the external force, we may require that the first one falls to U_1 in the next ratchet period, not the original one. Combining this new condition with the same condition C2 leads to a stronger sufficient condition for enhanced cooperativity of the form

$$\tfrac{1}{8}\alpha < \bar{\sigma} < 1 - \alpha. \tag{B6}$$

The line of reasoning sketched here for hard-core repulsion in the limit of vanishing noise can be generalized to obtain even less restrictive conditions, exact lower bounds for the velocity, and actually to compute the exact velocity-force curves for two motors by studying the whole tree of possibilities that may close the cycles with different displacements and time lapses. This study will be presented elsewhere [39].

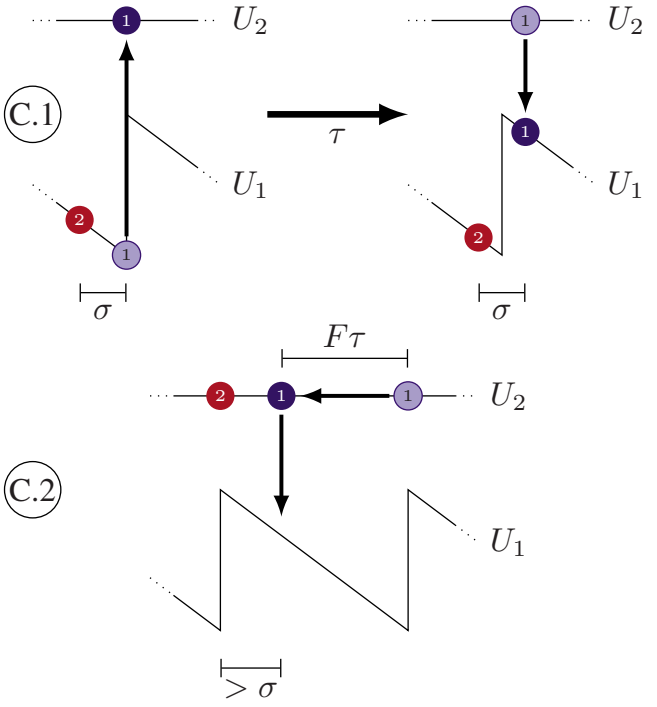

FIG. 24. (Color online) Schematic representation of the conditions needed to prove enhanced cooperativity. C1: starting with the two motors together in the bound state U_1, the first motor arrives to the transition zone and jumps to the weakly bound state U_2, and then both motors travel forward and after a time τ the first motor goes back to U_1 before the second one has reached the transition zone. C2: the first motor cannot interfere with the second one in the weakly bound state $F\tau < l - \sigma$.

[1] B. Alberts, A. Johnson, J. Lewis, M. Raff, K. Roberts, and P. Walter, *Molecular Biology of the Cell*, 4th ed. (Garland, New York, 1994).

[2] J. Howard, *Mechanics of Motor Proteins and the Cytoskeleton* (Sinauer Associates, Sunderland, MA, 2001).

[3] N. Hirokawa, Y. Noda, Y. Tanaka, and S. Niwa, Nat. Rev. Mol. Cell Biol. **10**, 682 (2009).

[4] F. Jülicher, A. Ajdari, and J. Prost, Rev. Mod. Phys. **69**, 1269 (1997).

[5] R. D. Astumian, Science **276**, 917 (1997).

[6] P. Reimann, Phys. Rep. **361**, 57 (2002).

[7] A. B. Kolomeisky and M. E. Fisher, Annu. Rev. Phys. Chem. **58**, 675 (2007).

[8] F. Jülicher and J. Prost, Phys. Rev. Lett. **78**, 4510 (1997).

[9] M. Badoual, F. Jülicher, and J. Prost, Proc. Natl. Acad. Sci. U.S.A. **99**, 6696 (2002).

[10] P.-Y. Plaçais, M. Balland, T. Guérin, J.-F. Joanny, and P. Martin, Phys. Rev. Lett. **103**, 158102 (2009).

[11] T. Guérin, J. Prost, P. Martin, and J.-F. Joanny, Curr. Opin. Cell Biol. **22**, 14 (2010).

[12] A. Kunwar and A. Mogilner, Phys. Biol. **7**, 016012 (2010).

[13] M. Vershinin, B. C. Carter, D. S. Razafsky, S. J. King, and S. P. Gross, Proc. Natl. Acad. Sci. U.S.A. **104**, 87 (2007).

[14] A. Roux, G. Cappello, J. Cartaud, J. Prost, B. Goud, and P. Bassereau, Proc. Natl. Acad. Sci. U.S.A. **99**, 5394 (2002).

[15] G. Koster, M. VanDuijn, B. Hofs, and M. Dogterom, Proc. Natl. Acad. Sci. U.S.A. **100**, 15583 (2003).

[16] C. Leduc, O. Campàs, K. Zeldovich, A. Roux, P. Jolimaitre, L. Bourel-Bonnet, B. Goud, J.-F. Joanny, P. Bassereau, and J. Prost, Proc. Natl. Acad. Sci. U.S.A. **101**, 17096 (2004).

[17] O. Campàs, Y. Kafri, K. B. Zeldovich, J. Casademunt, and J.-F. Joanny, Phys. Rev. Lett. **97**, 038101 (2006).

[18] O. Campàs, C. Leduc, P. Bassereau, J. Casademunt, J.-F. Joanny, and J. Prost, Biophys. J. **94**, 5009 (2008).

[19] P. M. Shaklee, T. Idema, G. Koster, C. Storm, T. Schmidt, and M. Dogterom, Proc. Natl. Acad. Sci. U.S.A. **105**, 7993 (2008).

[20] J. Tailleur, M. R. Evans, and Y. Kafri, Phys. Rev. Lett. **102**, 118109 (2009).

[21] C. Leduc, O. Campàs, J.-F. Joanny, J. Prost, and P. Bassereau, Biochim. Biophys. Acta **1798**, 1418 (2010).

[22] A. Parmeggiani, T. Franosch, and E. Frey, Phys. Rev. Lett. **90**, 086601 (2003).

[23] R. A. Blythe and M. R. Evans, J. Phys. A: Math. Theor. **40**, R333 (2007).

[24] C. Goldman and E. T. Sena, Physica A **388**, 3455 (2009).

[25] J. Brugués and J. Casademunt, Phys. Rev. Lett. **102**, 118104 (2009).

[26] A. Parmeggiani, F. Jülicher, A. Ajdari, and J. Prost, Phys. Rev. E **60**, 2127 (1999).

[27] J. M. R. Parrondo and B. J. de Cisneros, Appl. Phys. A: Mater. Sci. Process. **75**, 179 (2002).

[28] P. Hänggi, F. Marchesoni, and F. Nori, Ann. Phys. **14**, 51 (2005).

[29] N. Hirokawa and R. Takemura, Nat. Rev. Neurosci. **6**, 201 (2005).

[30] Y. Okada, H. Higuchi, and N. Hirokawa, Nature (London) **424**, 574 (2003).

[31] Y. Okada, H. Yamazaki, Y. Sekine-Aizawa, and N. Hirokawa, Cell **81**, 769 (1995).

[32] G. B. Stokin *et al.*, Science **307**, 1282 (2005).

[33] D. Oriola, J. G. Orlandi, and J. Casademunt (unpublished).

[34] I. Derényi and A. Ajdari, Phys. Rev. E **54**, R5 (1996).

[35] F. Slanina, J. Stat. Phys. **135**, 935 (2009).

[36] With constant decay time, the problem is in fact non-Markovian for time scales on the order of τ. In addition this also breaks the local detailed balance condition usually assumed for molecular motors.

[37] In the discrete model of [17] this scaling is only found exceptionally for the stall force, but for any finite velocity in the limit of large N the velocity-force relation converges to a single curve independent of N.

[38] Note that the MF assumption here has a different meaning from other approximations under this name that neglect fluctuations for large numbers of motors, such as, for instance, those in Refs. [8,10,35].

[39] C. Blanch-Mercader, J. G. Orlandi, and J. Casademunt (unpublished).

[40] S. Klumpp, A. Mielke, and C. Wald, Phys. Rev. E **63**, 031914 (2001).

[41] S. Klumpp and R. Lipowsky, Proc. Natl. Acad. Sci. U.S.A. **102**, 17284 (2005).

[42] M. Evstigneev, S. von Gehlen, and P. Reimann, Phys. Rev. E **79**, 011116 (2009).

[43] Y. Okada and N. Hirokawa, Science **283**, 1152 (1999).

[44] N. Hirokawa, R. Nitta, and Y. Okada, Nat. Rev. Mol. Cell Biol. **10**, 877 (2009).

[45] P. Greulich, A. Garai, K. Nishinari, A. Schadschneider, and D. Chowdhury, Phys. Rev. E **75**, 041905 (2007).

[46] D. R. Klopfenstein, M. Tomishige, N. Stuurman, and R. D. Vale, Cell **109**, 347 (2002).

[47] J. Helenius, G. Brouhard, Y. Kalaidzidis, S. Diez, and J. Howard, Nature (London) **441**, 115 (2006).

[48] C. Kaether, P. Skehel, and C. G. Dotti, Mol. Biol. Cell **11**, 1213 (2000).

[49] A. Parmeggiani, F. Jülicher, L. Peliti, and J. Prost, EPL **56**, 603 (2001).

[50] W. H. Roos, O. Campàs, F. Montel, G. Woehlke, J. P. Spatz, P. Bassereau, and G. Cappello, Phys. Biol. **5**, 046004 (2008).

[51] J. M. Scholey, Dev. Cell **2**, 515 (2002).

[52] J. Buceta, J. M. Parrondo, C. Van den Broeck, and F. J. de la Rubia, Phys. Rev. E **61**, 6287 (2000).

[53] I. Minoura, E. Katayama, K. Sekimoto, and E. Muto, Biophys. J. **98**, 1589 (2010).